Dilute Magnetic Topological Insulators

Laurens W. Molenkamp

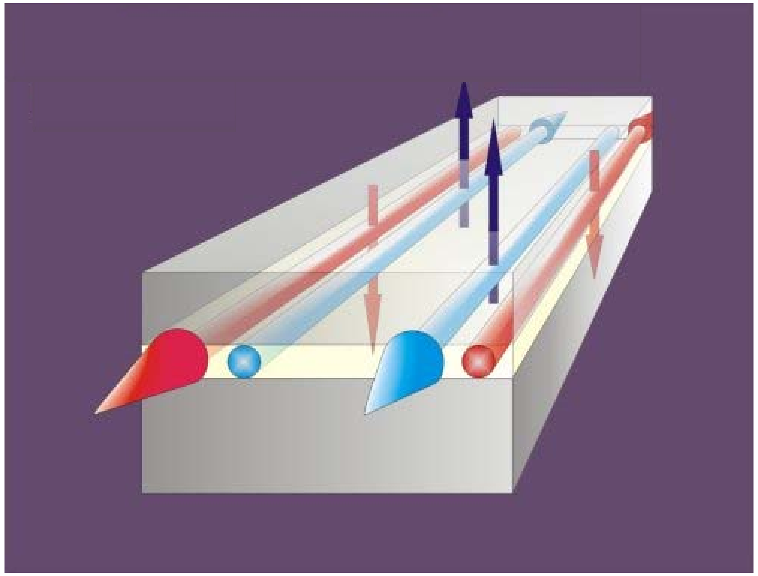

EP III and Institute for Topological Insulators
Würzburg University

Outline

- HgTe quantum wells alloyed with Mn atoms
- Quantized spin Hall conductance in Mn-doped HgTe: Kondo screening
- Emergent quantum Hall phenomena
  - ✓ QSH states when time reversal symmetry is broken
  - ✓ Effect of enhanced DOS in valence band
- In 3-D TI: parity anomaly
- Proximitized layers: FFLO-type superconductivity

The quantum spin Hall effect

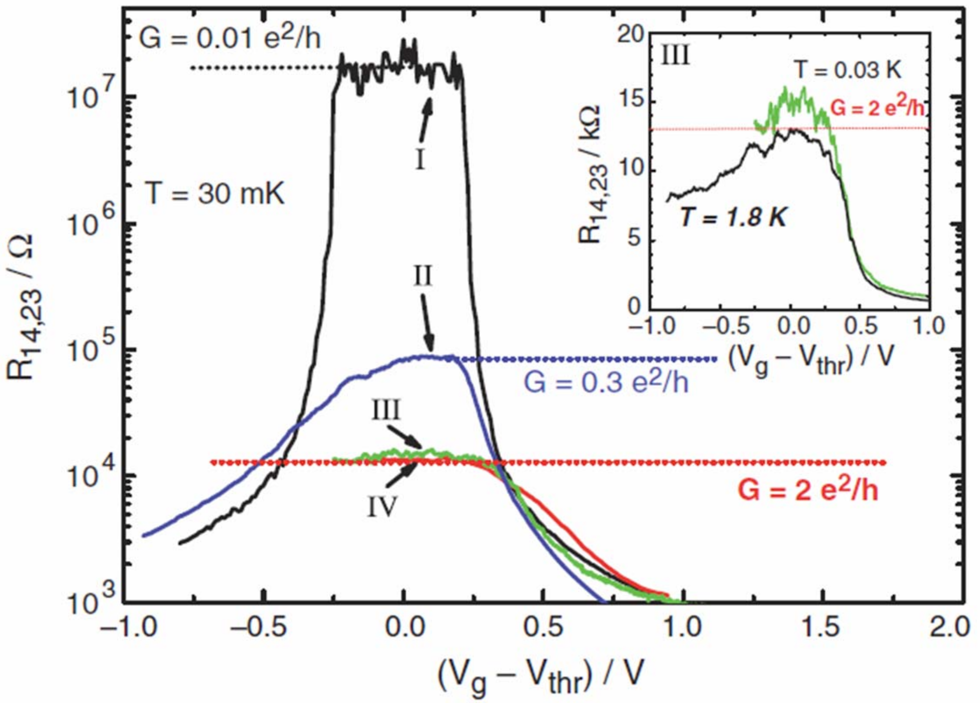

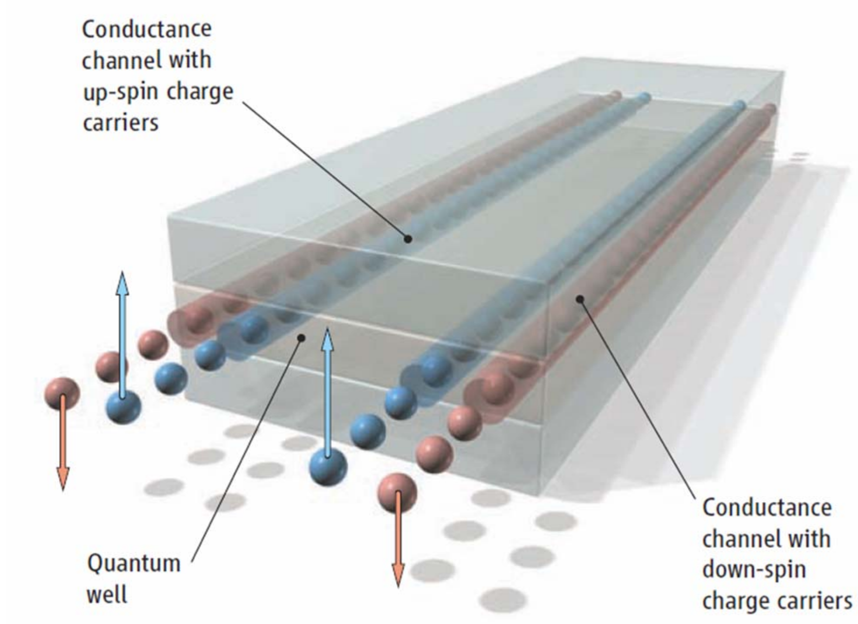

Some recent insights….

M. König, *et. al. Science* **318**, 766 (2007)

BHZ model (over) simplifies HgTe band structure

B.A Bernevig, T.L. Hughes, S.C. Zhang, Science **314**, 1757 (2006)

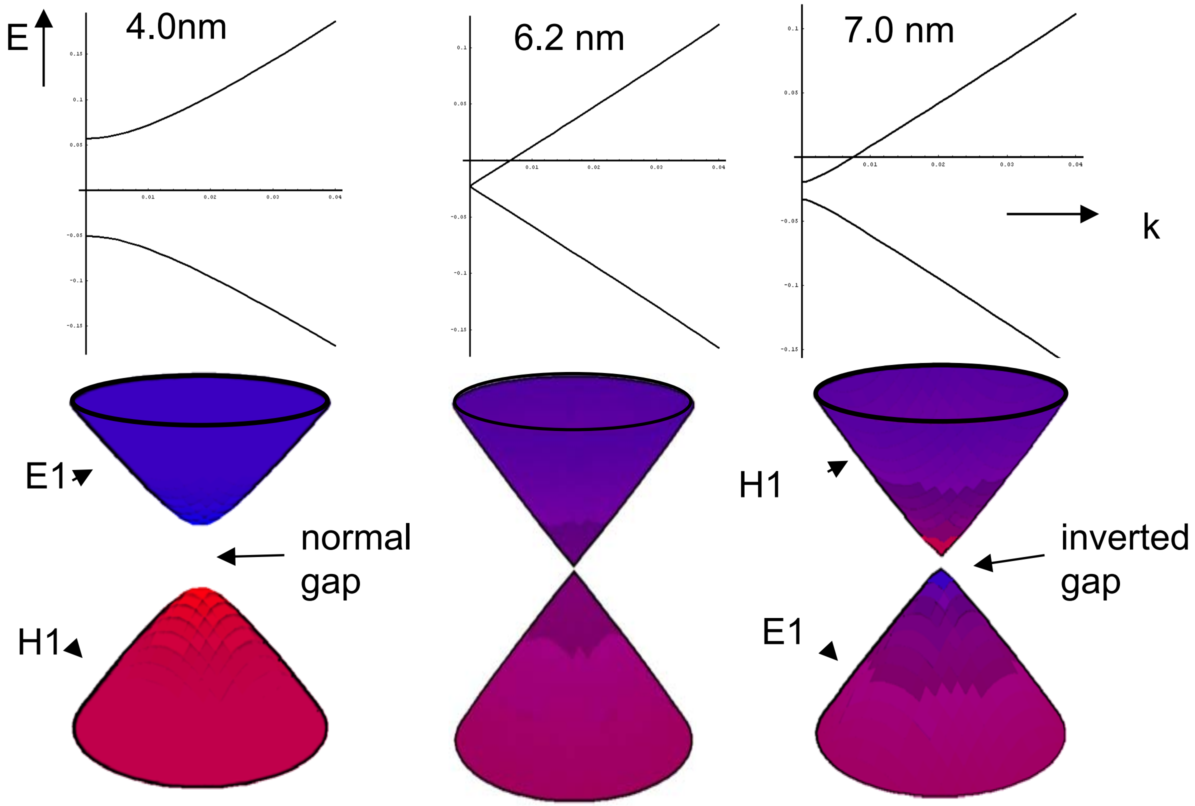

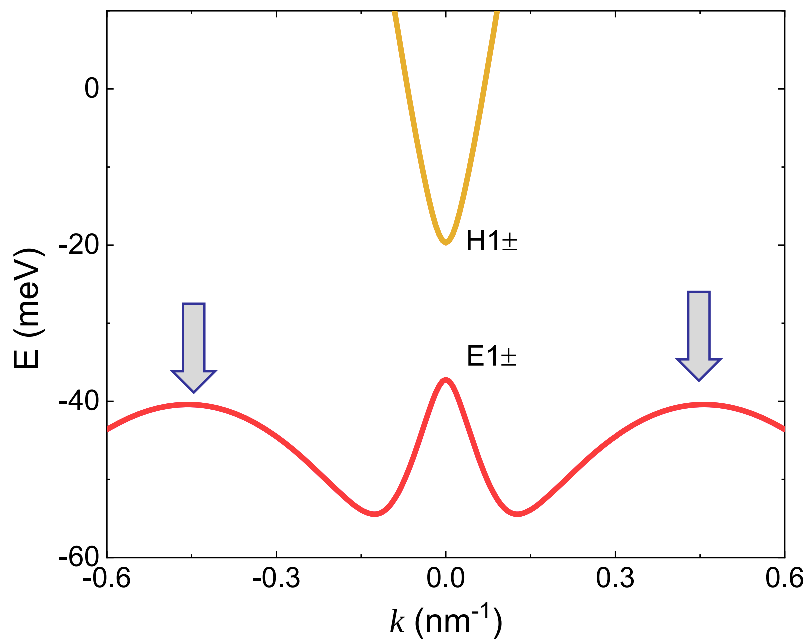

- ‘Camelback’ van Hove singularity is absent in BHZ model

Two recent developments in sample treatment

NANO LETTERS Letter
Cite This: *Nano Lett.* 2018, 18, 4831–4836 pubs.acs.org/NanoLett

High Mobility HgTe Microstructures for Quantum Spin Hall Studies

- Wet etching of nanostructures to avoid sample damage

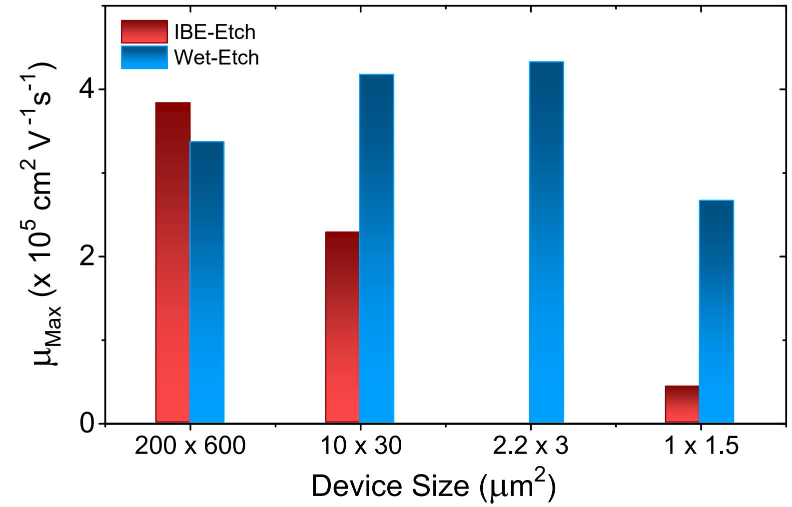

PHYSICAL REVIEW LETTERS **123,** 047701 (2019)
Editors' Suggestion

Approaching Quantization in Macroscopic Quantum Spin Hall Devices through Gate Training

- Gate training reduces puddle disorder
- Increases scattering length to ca. 100 μm

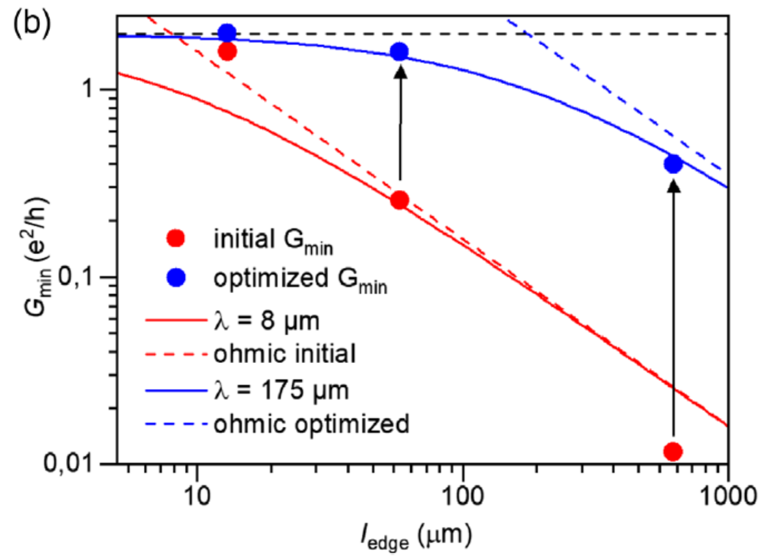

Wet etching of Nanostructures

Wet etched micron-sized hall bars show strongly improved transport properties;
better mobilities and better quantum Hall effect (homogeneity)

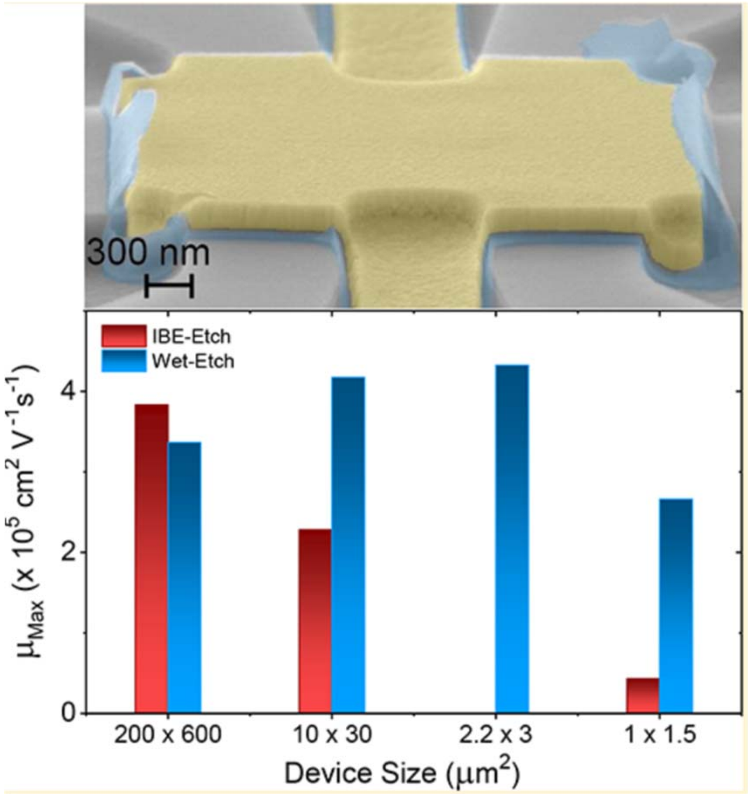

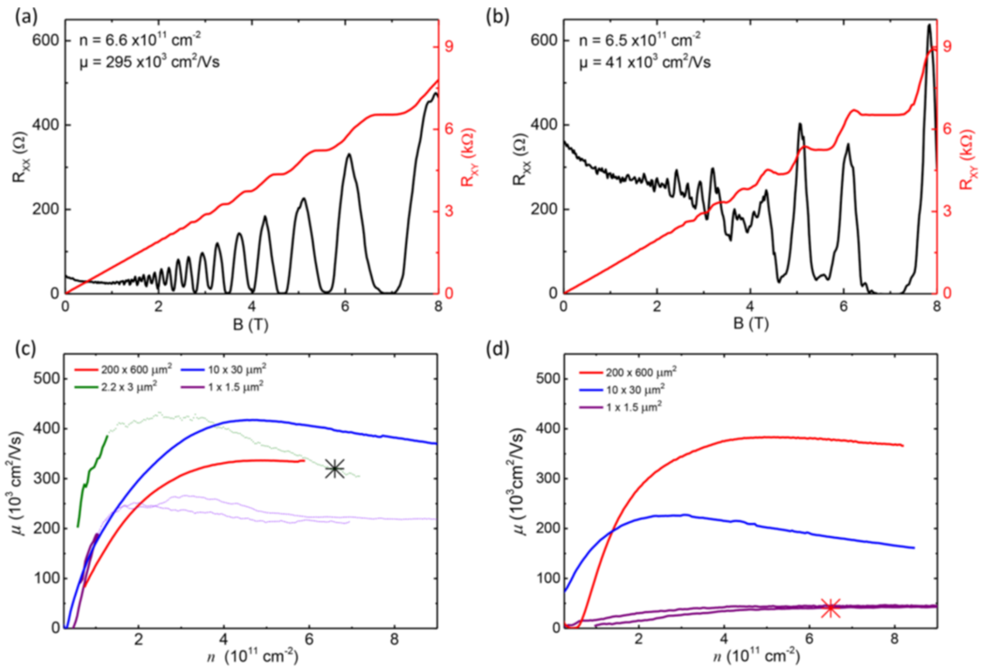

K. Bendias et al., Nano Lett. **18**, 4831, 2018

Wet etching….

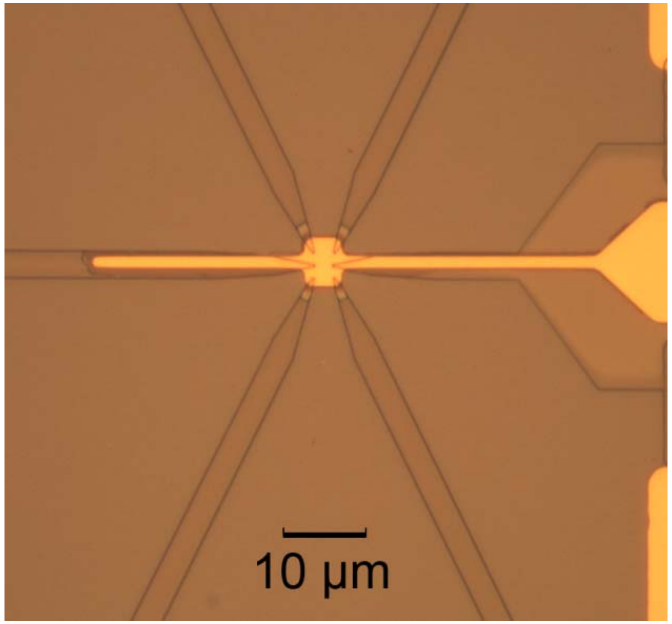

K. Bendias et al., Nano Lett. 10.1021, 2018

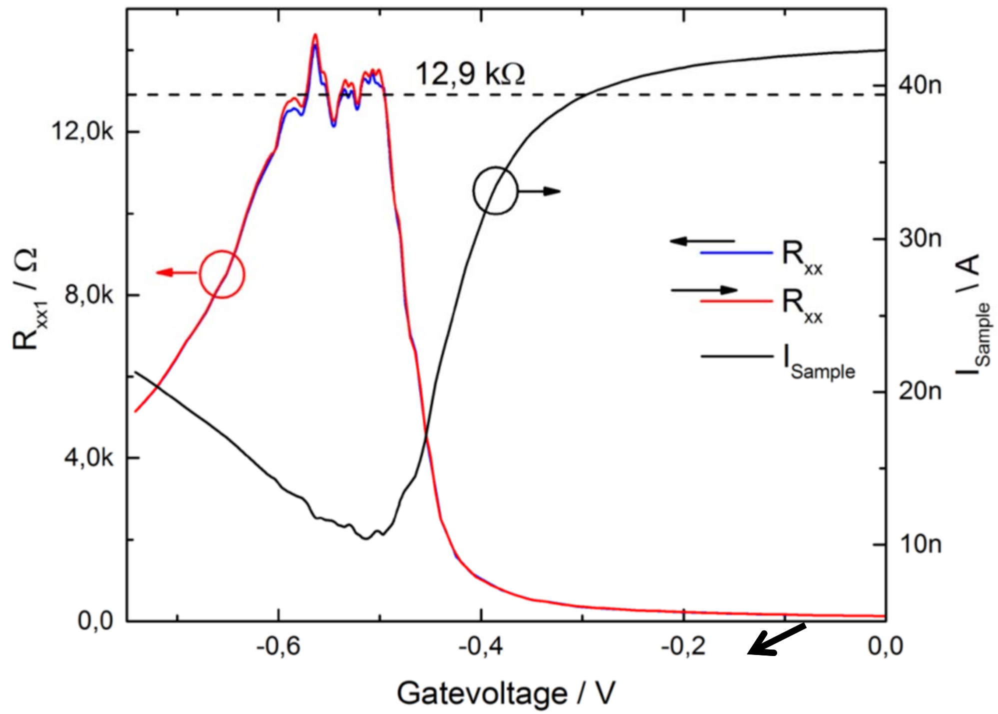

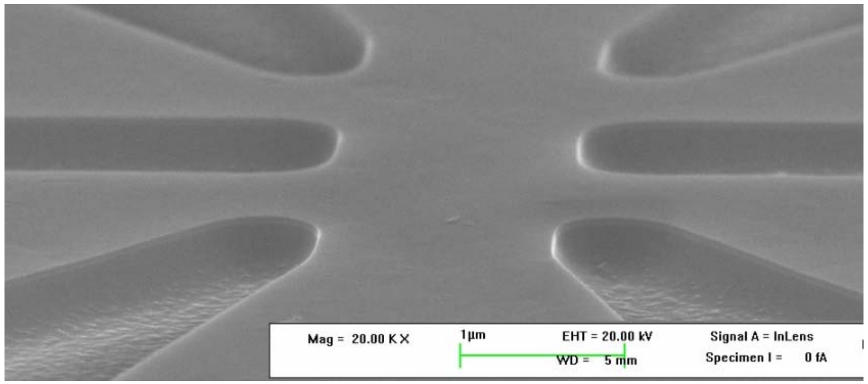

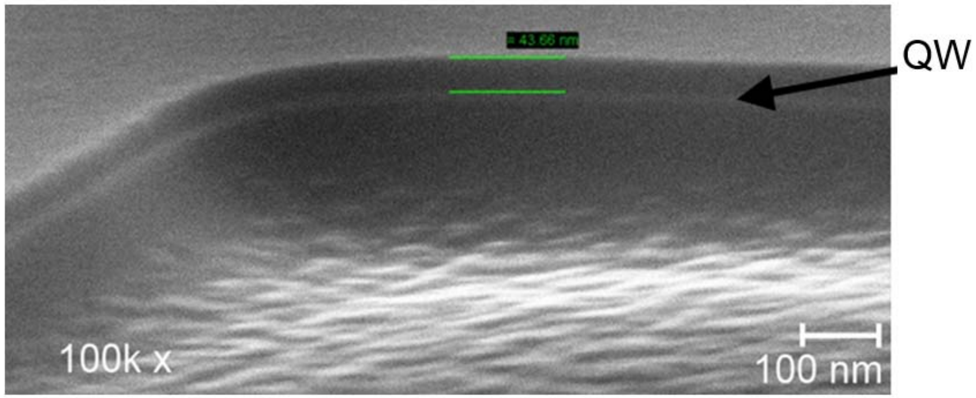

Gate Training in large Hall bars

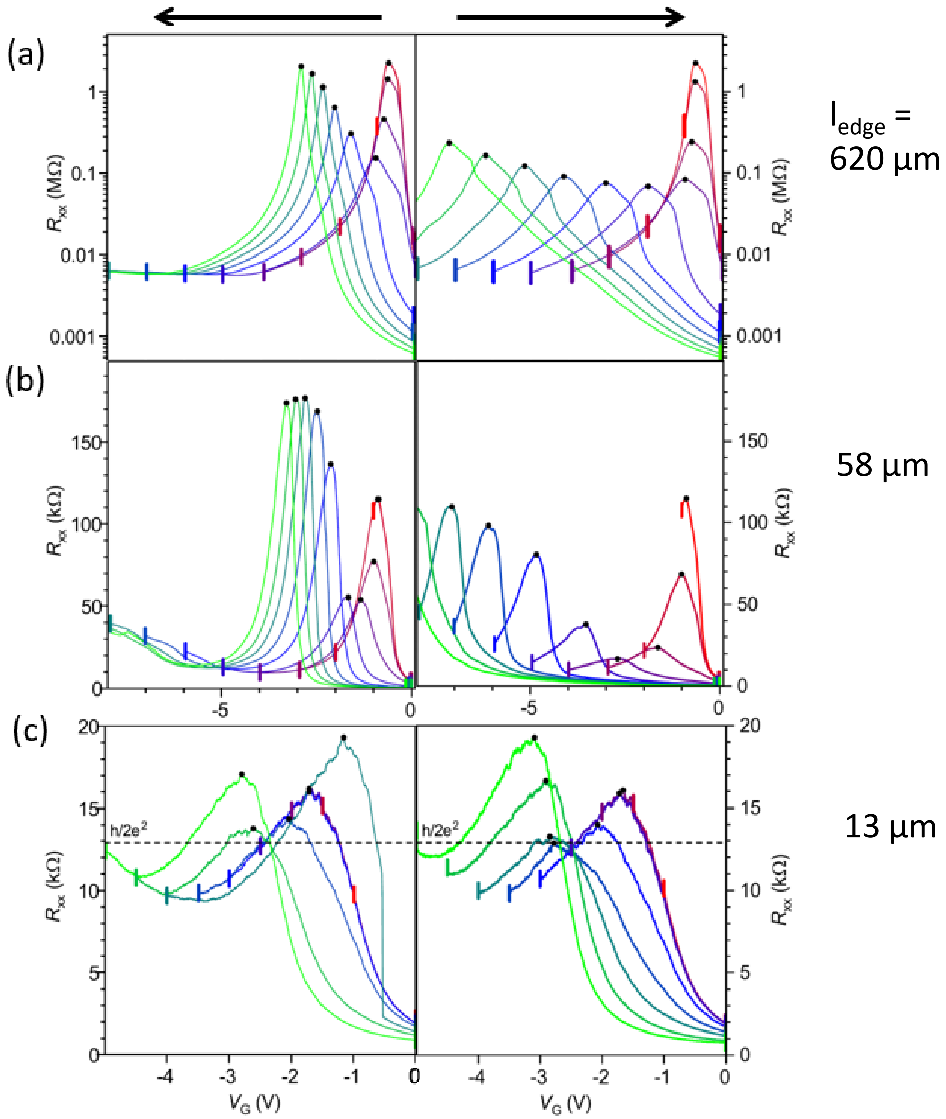

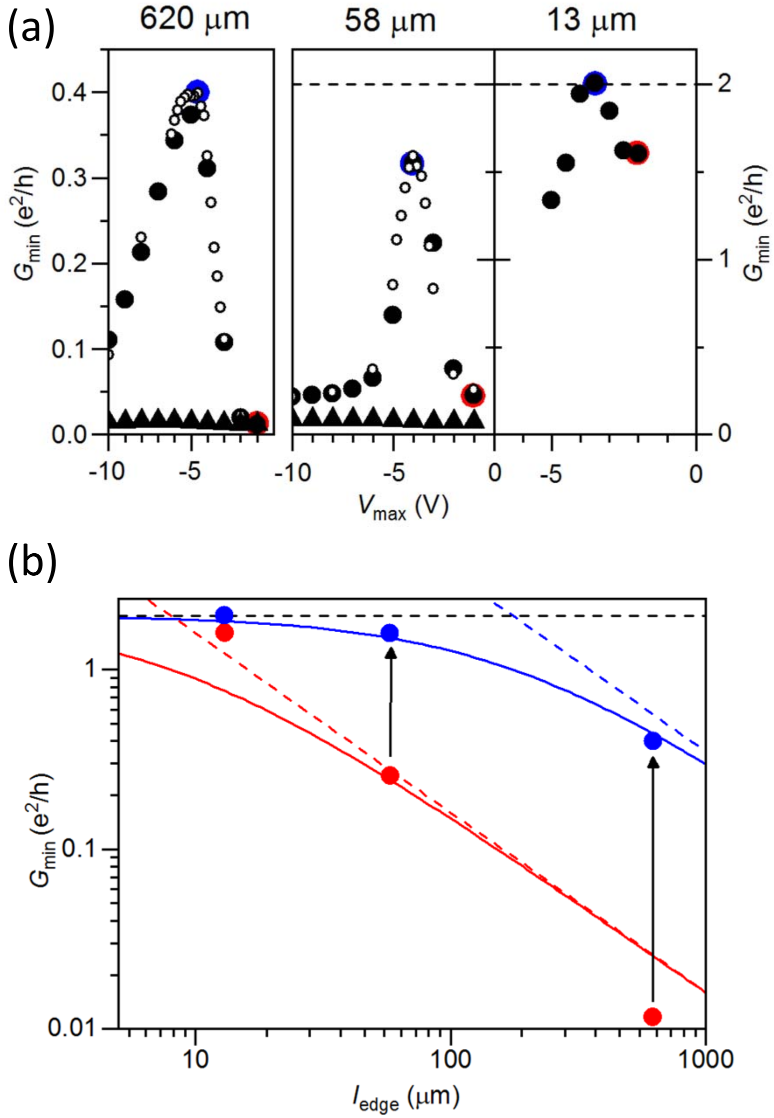

L. Lunczer et al., Phys. Rev. Lett. **123**, 047701 (2019).

(Hg,Mn)Te layers

- The Mn atoms substitute Hg atoms isoelectrically: dilute magnetic II-VI semiconductor
- No change in carrier concentration; no degradation of device quality and no ferromagnetism, bandstructure influence is similar to other IIs
- Chemical composition: $\mathrm{Hg_{1-x}Mn_xTe}$; x is in the range $0.01 - 0.025$
- For the above concentration of Mn atoms, (Hg,Mn)Te QWs are paramagnetic; the magnetization is zero in the absence of an external magnetic field
- Giant Zeeman effect: at finite B, the magnetization can be calculated as $\langle m \rangle = -S_0 \frac{\vec{B}}{B} B_{5/2}\left(\frac{5}{2}\frac{g_{Mn}\mu_B B_T}{k_B(T+T_0)}\right)$
- g-factor enhanced through this magnetization (follows same Brillouin function.)
- Typical n density $\sim 10^{11} - 10^{12}\ \mathrm{cm^{-2}}$, typical mobility $\sim 2 \times 10^5\ \mathrm{cm^{-2}V^{-1}s^{-1}}$

Questions

- Can we observe the quantized conductance when we add magnetic impurities?
- Effect of magnetic field on the edge channels – Do the edge channels survive the breakdown of time reversal symmetry
- Effect of the van Hove singularity in the valence band?

Topological phase space of (Hg,Mn)Te QWs

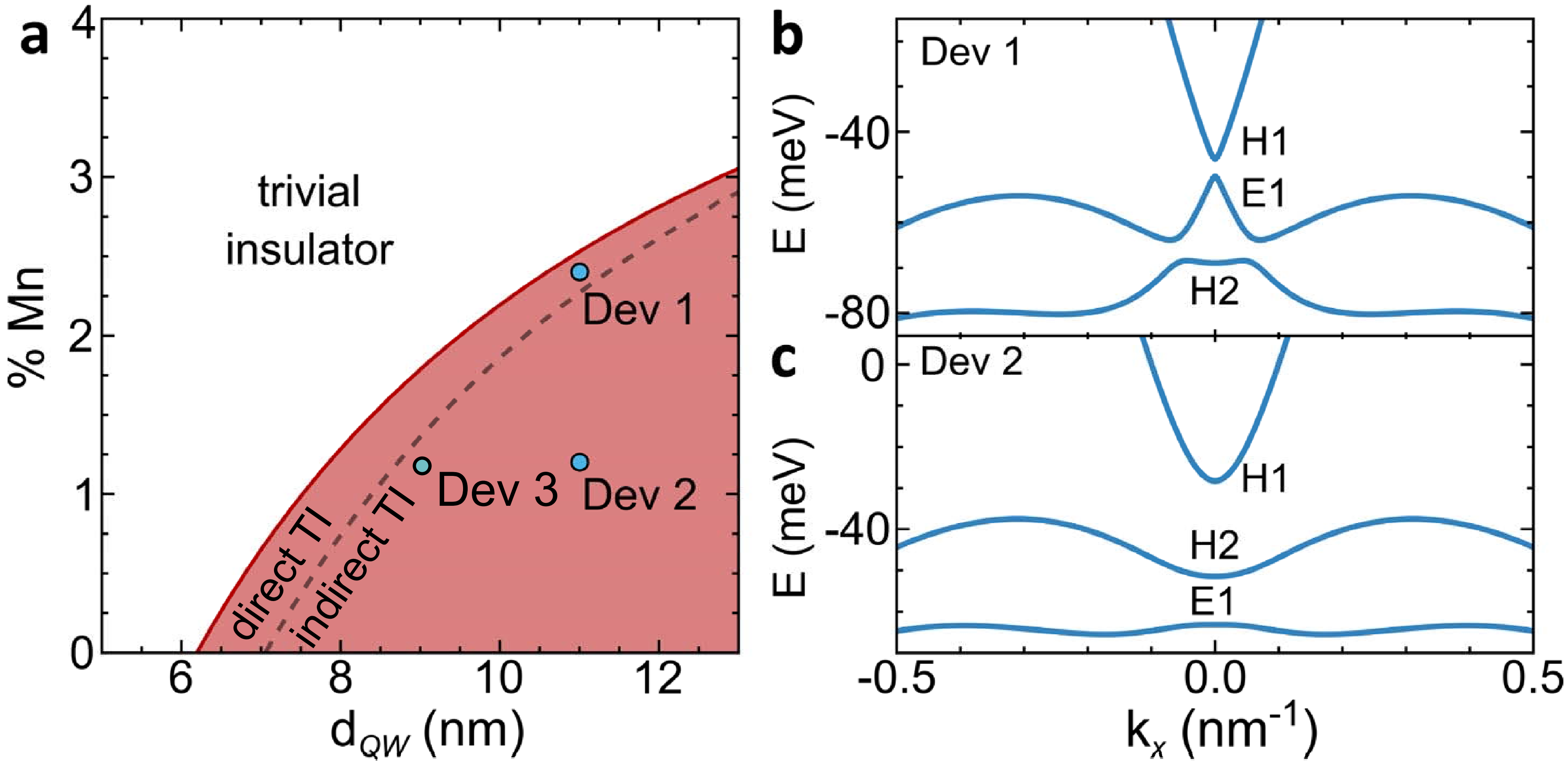

S. Shamim et al., *Science Advances* **6**, eaba4625 (2020).

Breaking Time Reversal Symmetry in a Topological Insulator

- Will adding magnetic impurities destroy the quantum spin Hall effect ?

- Very different predictions about fate of the quantum spin Hall effect in the presence of magnetic impurities (can cause spin-flip scattering and break local time reversal symmetry):

- No effect (Tanaka et al., PRL 2011)
- Anderson localization (Altshuler et al., PRL 2013)
- Kondo screening (Maciejko et al., PRL 2009)

Quantized spin Hall conductance in (Hg,Mn)Te QWs

Dev 3: 9 nm QW, 1.2% Mn

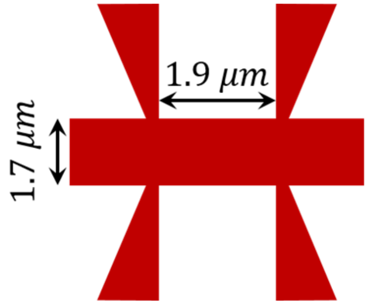

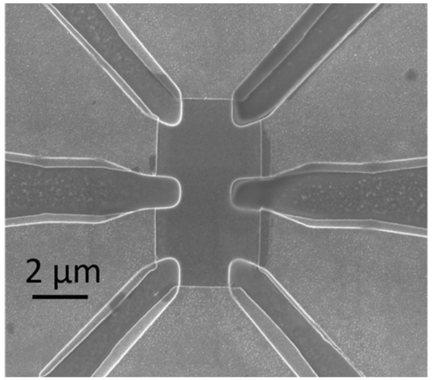

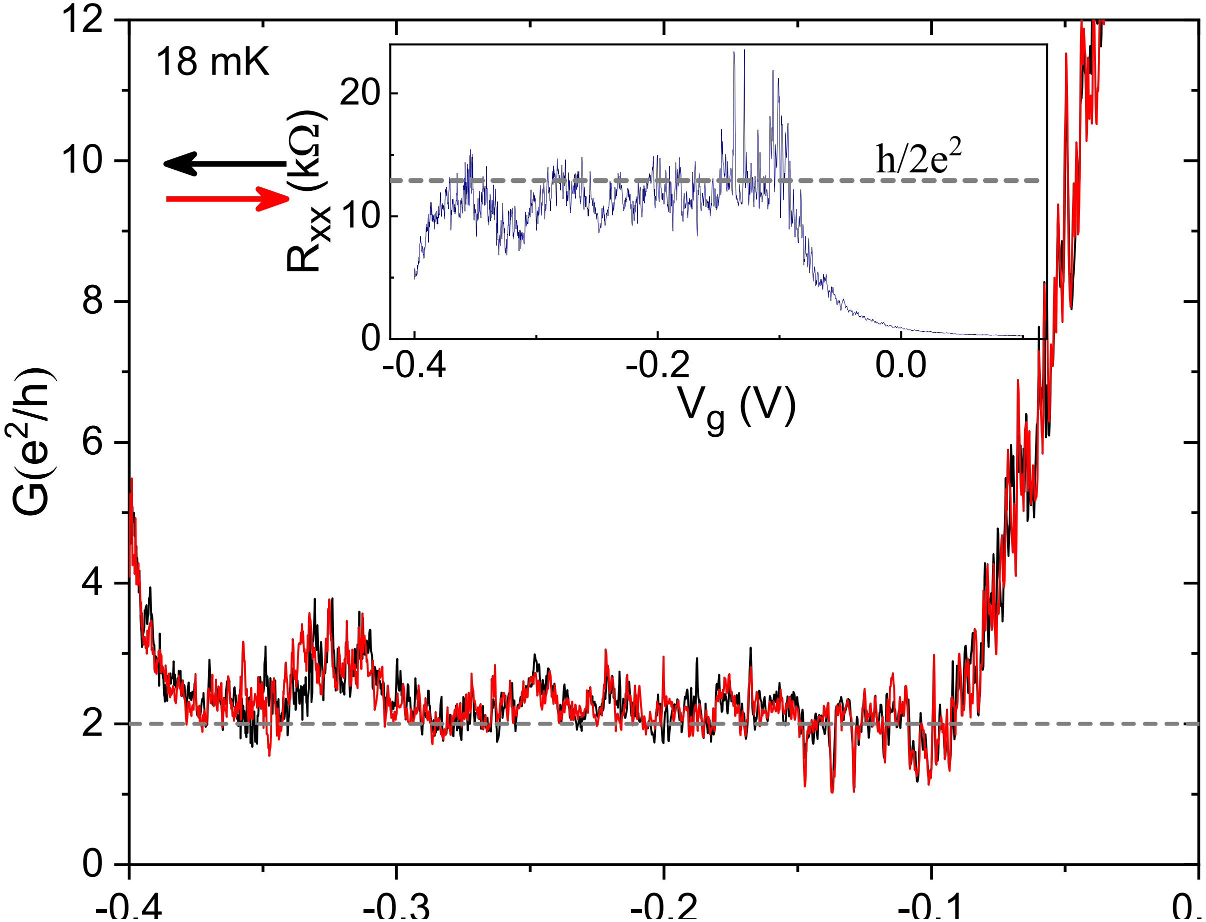

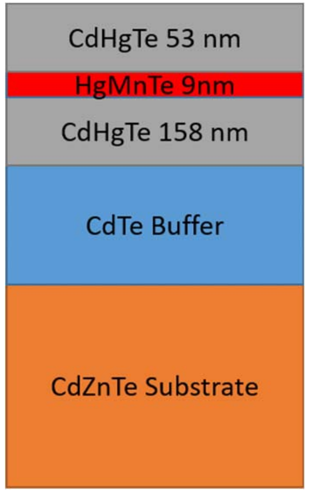

- After gate training, we observe clear conductance quantization of the quantum spin Hall effect in the presence of magnetic impurities.
- Very long plateau due to camelback

S. Shamim et al., Nature Comm. **12**, 3193 (2021).

Quantization recovered only at low temperatures

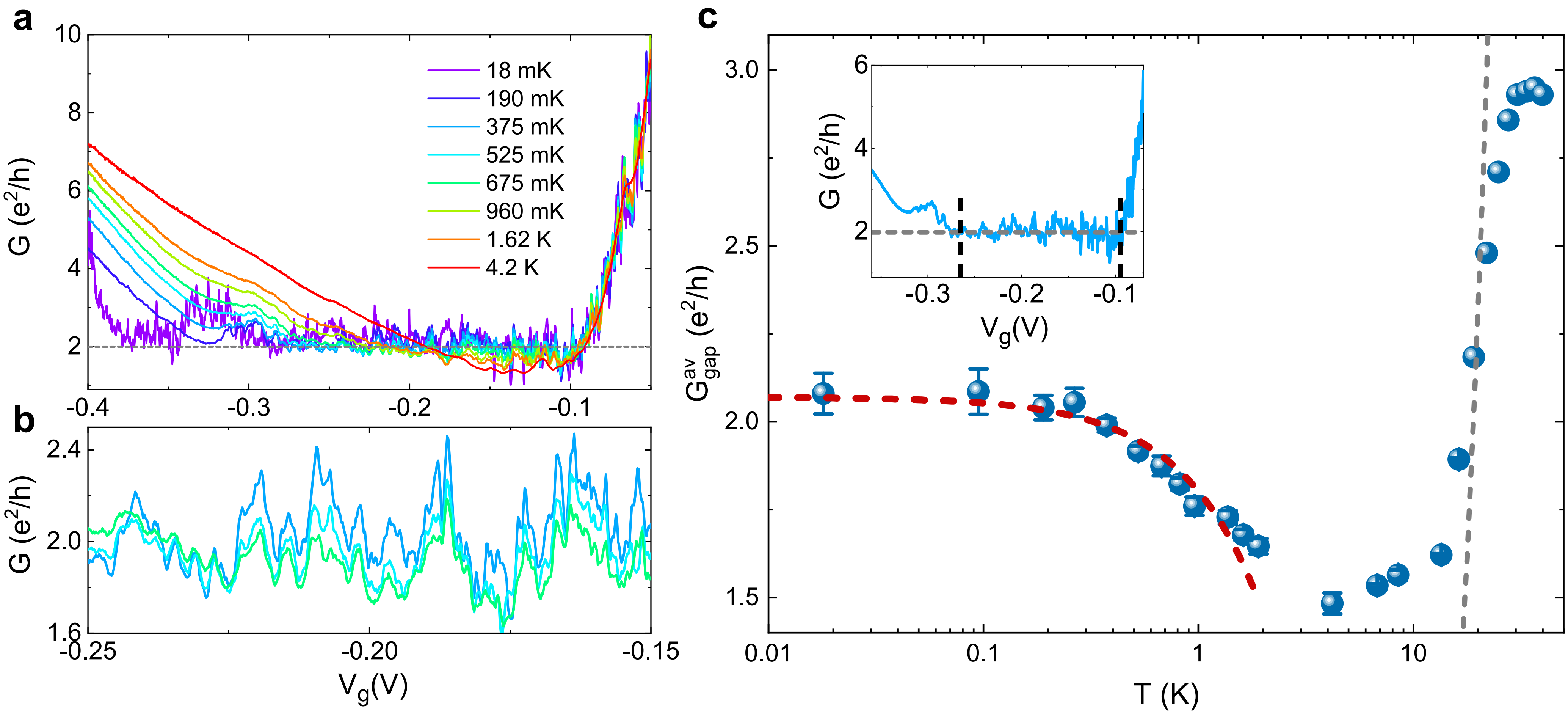

Low temperature behavior suggests Kondo screening of the magnetic impurity at low temperature.

Thermal activation of plateau width: Camelback in valence band

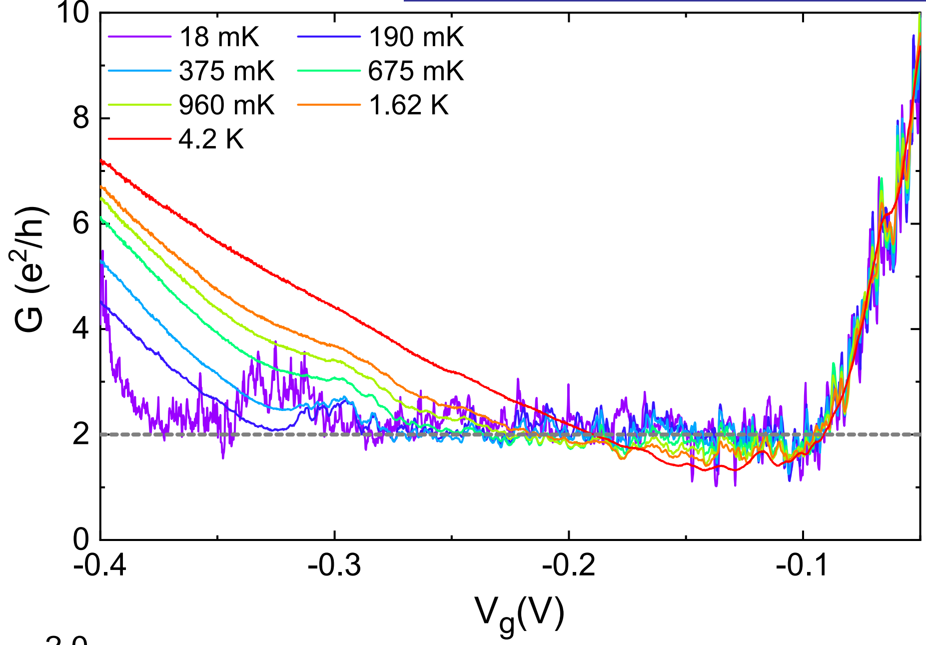

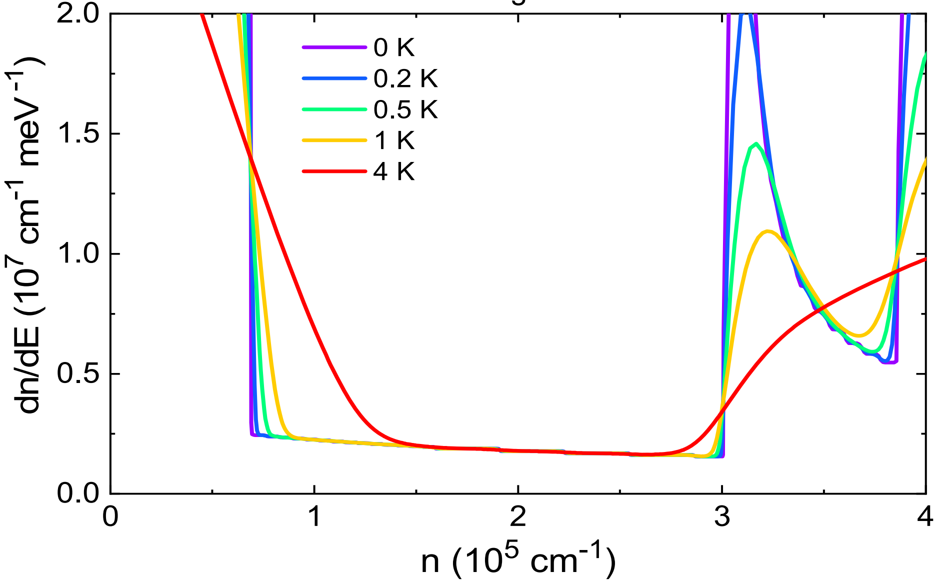

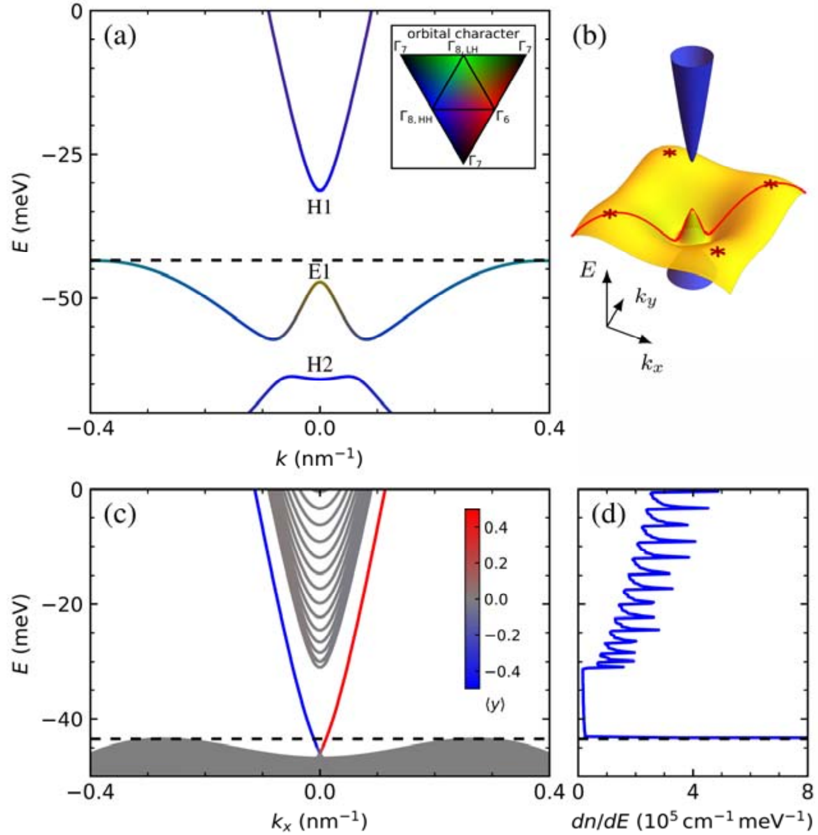

Wouter Beugeling

Kondo Screening

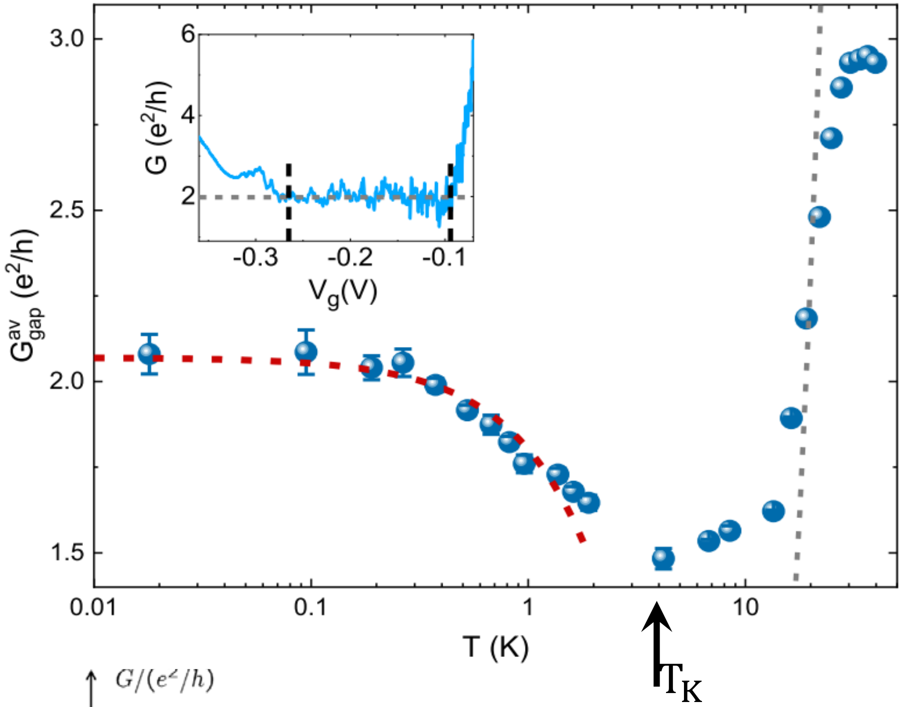

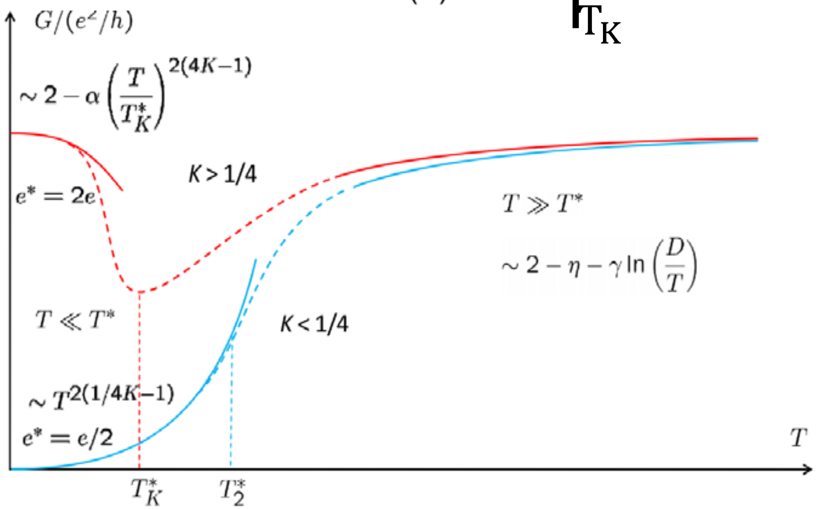

Comparison with theory by Maciejko *et. al.*, *PRL* **102**, 256803 (2009).

Interaction parameter

$$K = \left[1 + \frac{2}{\pi}\frac{e^2}{\epsilon_0 \epsilon_r \hbar v_F} \ln\left(\frac{7.1d}{\xi + 0.8w}\right)\right]^{-1/2} \sim 0.5.$$

Assumes isotropic scattering.

High temperature activation simply results from thermal across-gap excitation

Breaking Time Reversal Symmetry in a Topological Insulator

- Adding magnetic impurities does not destroy the quantum spin Hall effect
- What will a magnetic field do, i.e. global breaking of time reversal symmetry?

Emergence of QH states from QSH states

Dev 3: 9 nm QW, 1.2% Mn

Quantum spin Hall effect at B = 0T characterized by $R_{XX} = \frac{h}{2e^2}$ and $R_{XY} = 0$

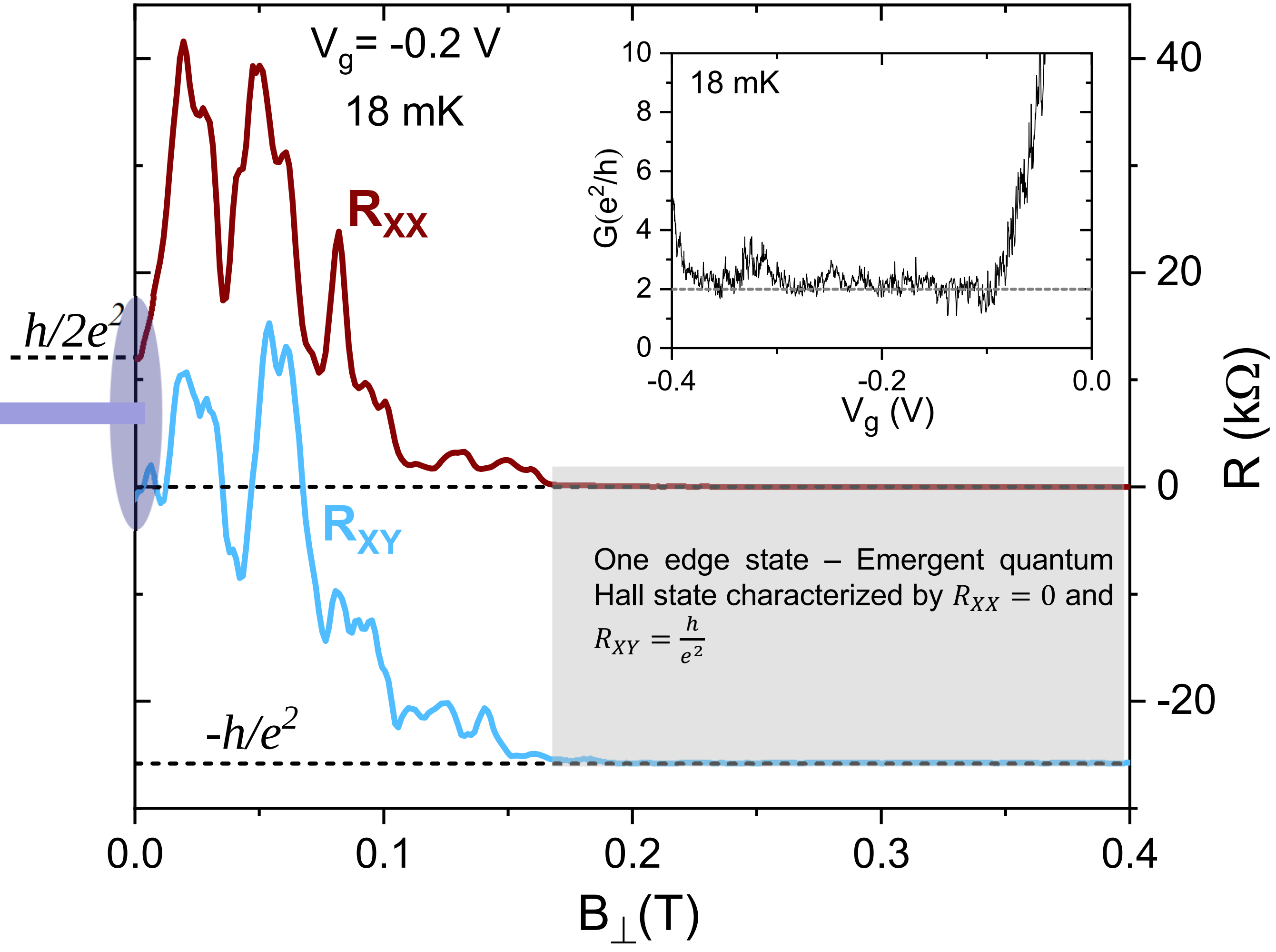

- Onset of $\nu = -1$ plateau at ***unexpectedly low*** perpendicular magnetic field

Emergence of QH effect from QSH edge states

Dev 1: 11 nm QW, 2.4% Mn

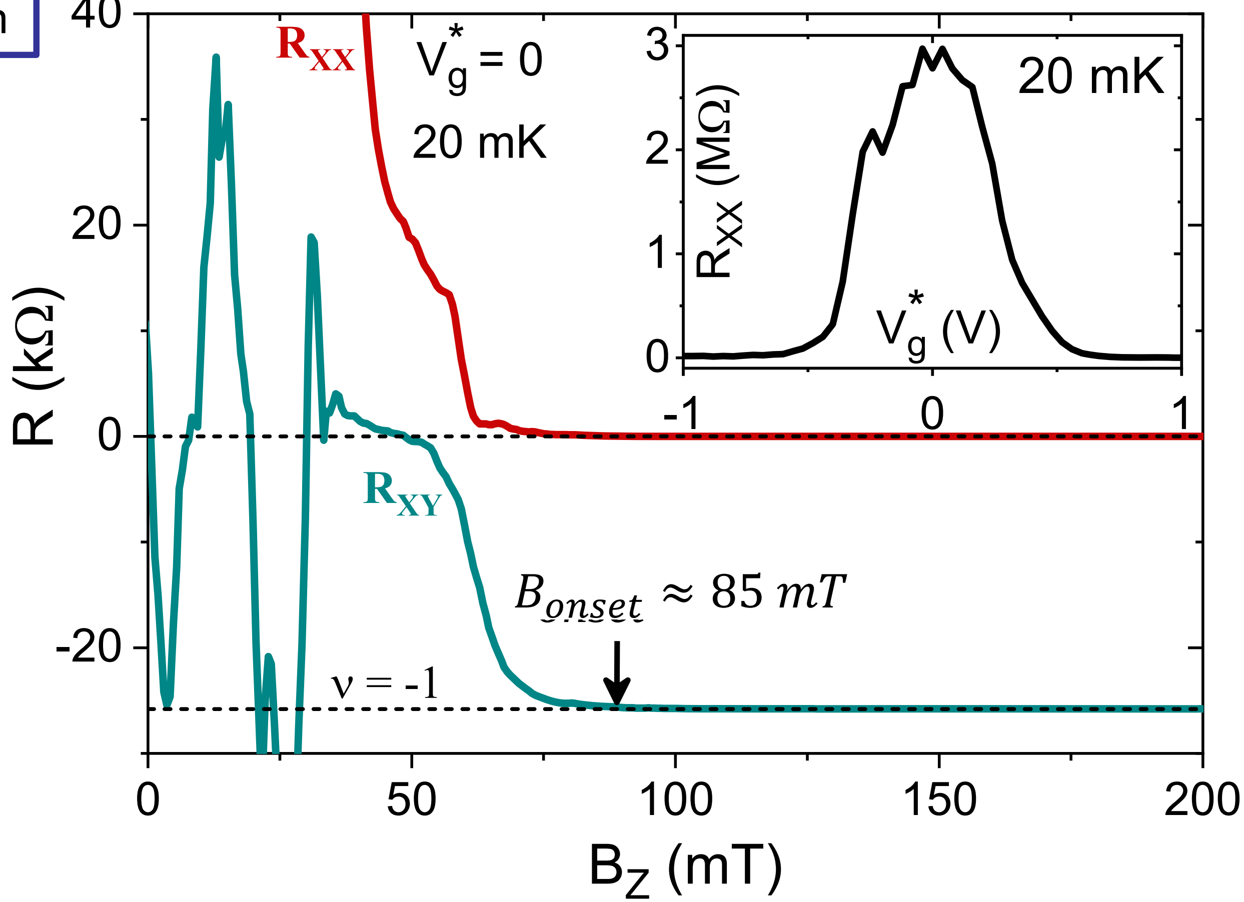

- Macroscopic Hall bar (600 x 200 μm^2), 11 nm (Hg,Mn)Te QW with 2.4% Mn
- Not quantized at zero field because of large device dimensions
- More suited to explore various aspects of QHE in (Hg,Mn)Te due to cleaner Hall signal in large device
- Onset of $\nu = -1$ plateau at unexpectedly low perpendicular magnetic field

S. Shamim et al., Sci. Adv. **6**, eaba4625 (2020).

Emergence of QH effect from QSH states

Dev 1: 11 nm QW, 2.4% Mn

- Influence of gate voltage on $\nu = -1$ plateau

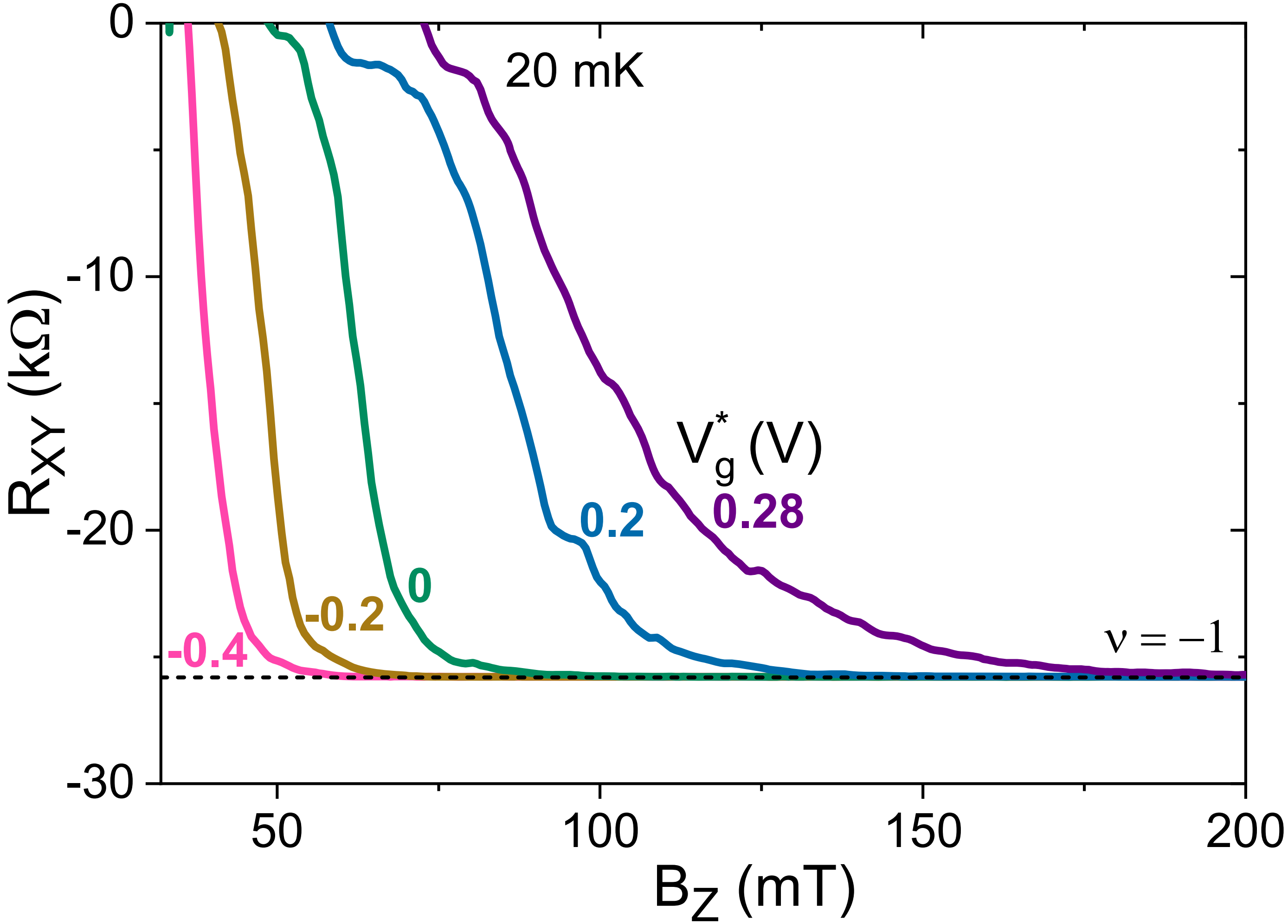

S. Shamim et al., Sci. Adv. **6**, eaba4625 (2020).

Onset too early for QAHE in (Hg,Mn)Te

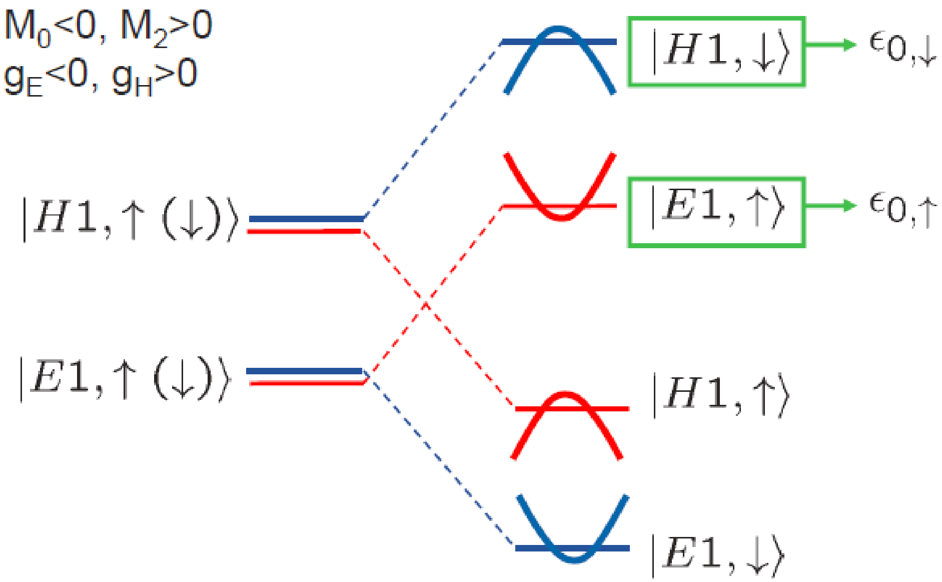

Phys. Rev. Lett. **101**, 146802 (2008)

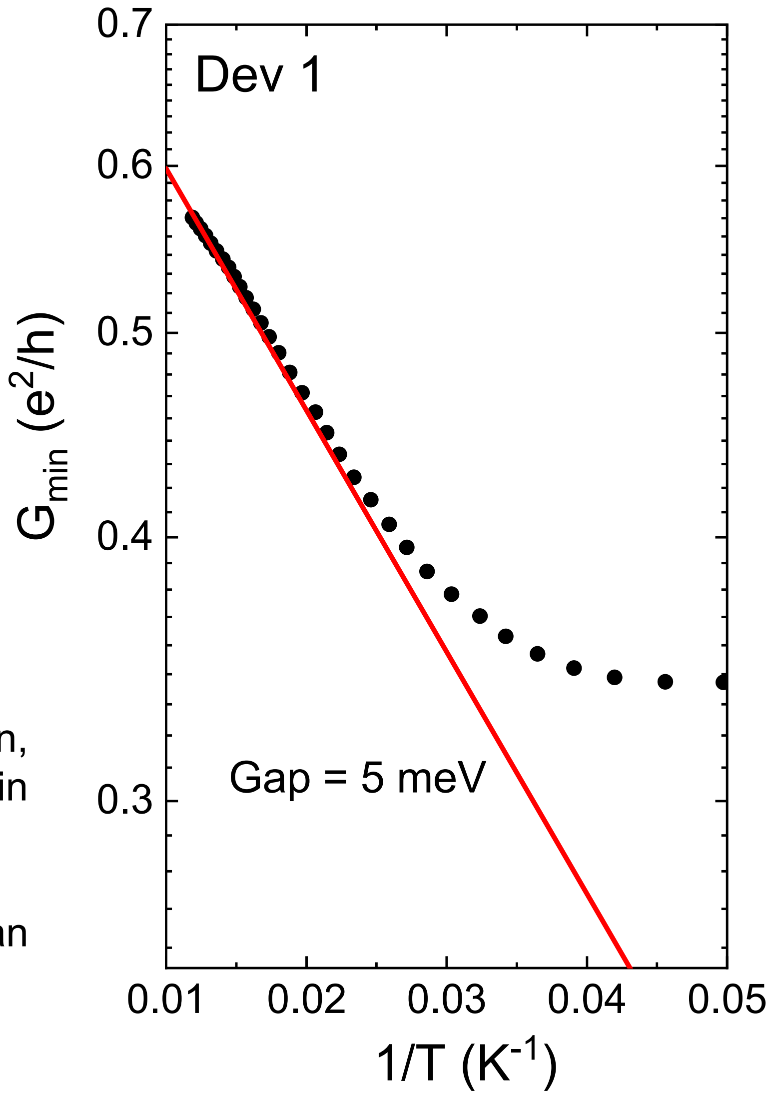

- From C. X. Liu et al., PRL 101, 146802 (2008), for 2% Mn, magnetization $\langle S\rangle > 0.5$ need to close the gap for realizing the QAHE in HgMnTe
- Here, the onset occurs at $B_\perp \approx 0.1$ T, corresponding to $\langle S\rangle \approx 0.15$; can close a gap of 1meV
- Different mechanism at play!! ⇒ Back to k.p calculations

k.p on a strip: Effect of perpendicular magnetic field

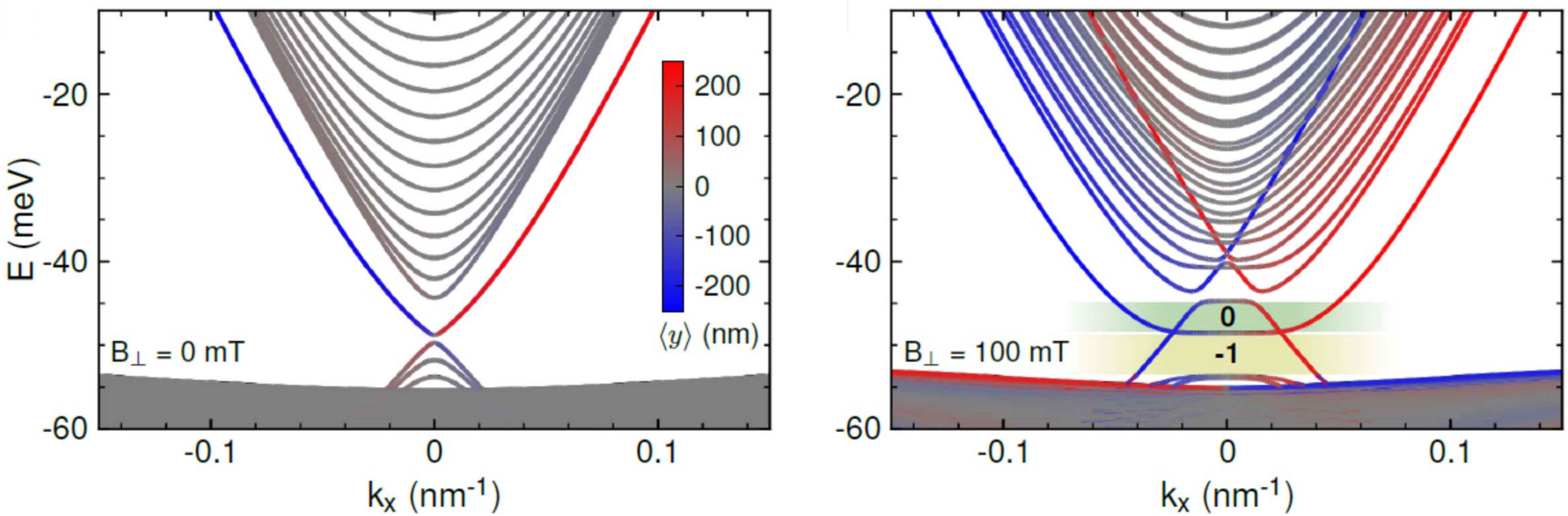

Calculations: W. Beugeling

- At zero field, Dirac point is just above camel's back.
- At finite fields, one spin state shifts down, leaves the topological gap and hybridizes with large dos at camel's back.
- The other shifts up and remains unhybridized with cb bulk states (different k value)
- Emergent $\nu = -1$ QH state in the LL gap

One quantum spin Hall edge channel survives the breakdown of time reversal symmetry

S. Shamim et al., Sci. Adv. **6**, eaba4625 (2020).

Next, we tune the Fermi level into the bulk valence band

Dev 1: 11 nm QW, 2.4% Mn

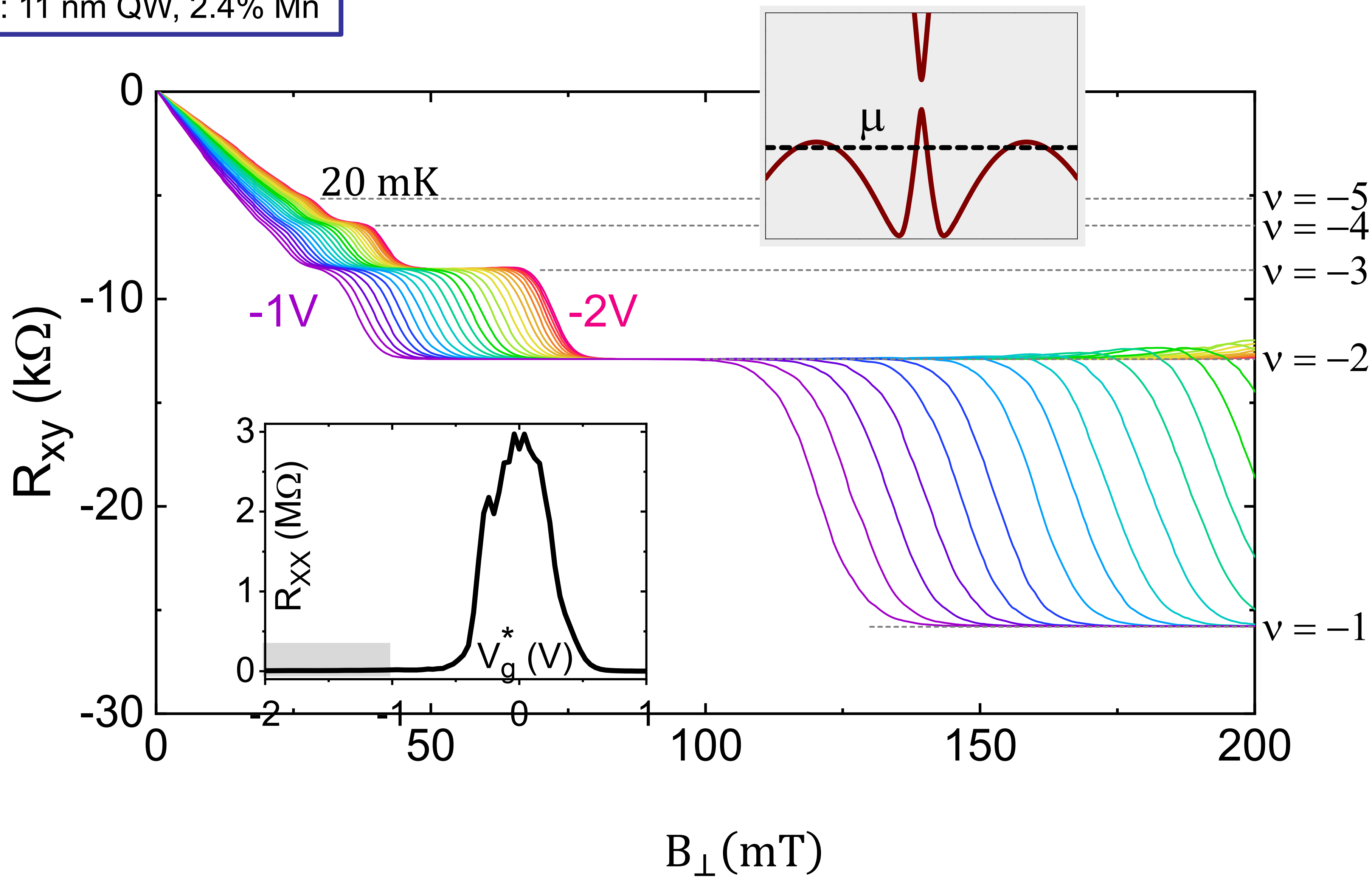

Highly mobile holes near k=0

Dev 1: 11 nm QW, 2.4% Mn

Expected carrier density, from the gate efficiency - $5 \times 10^{11}\ \mathrm{cm}^{-2}$

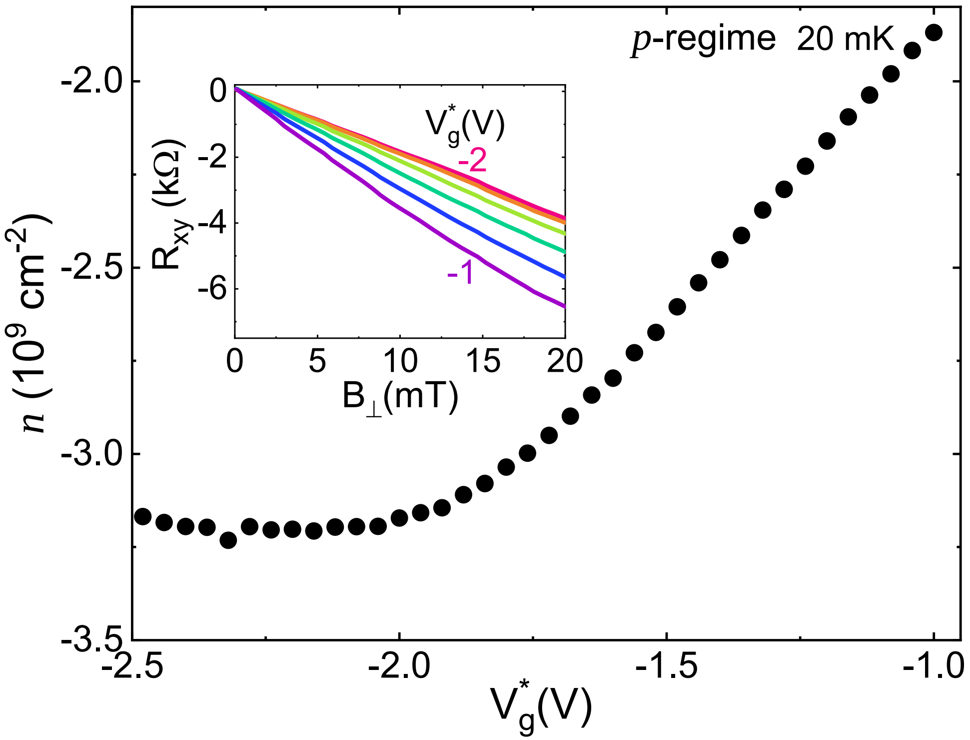

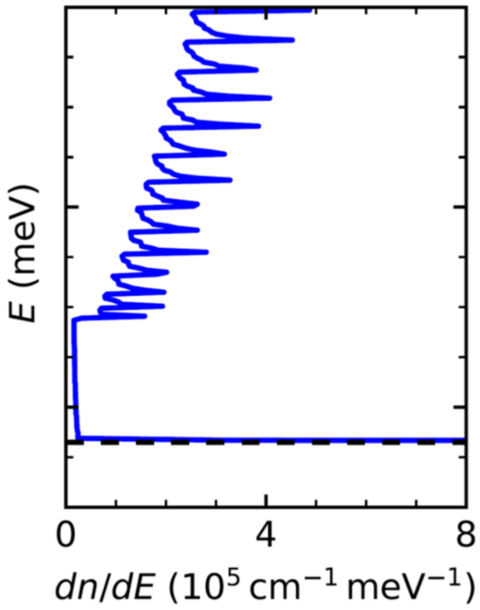

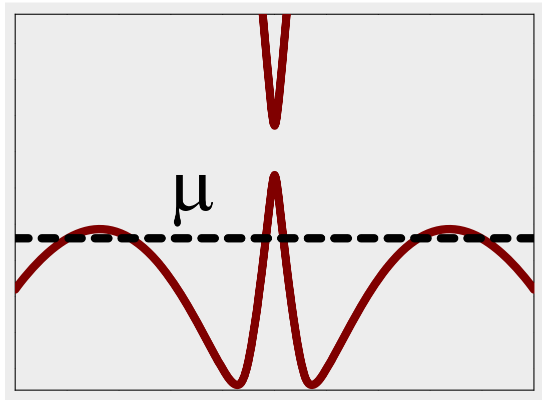

Localized carriers at the *camelback*

Highly mobile holes near k=0

Dev 1: 11 nm QW, 2.4% Mn

Expected carrier density, from the gate efficiency - $5 \times 10^{11}\ cm^{-2}$

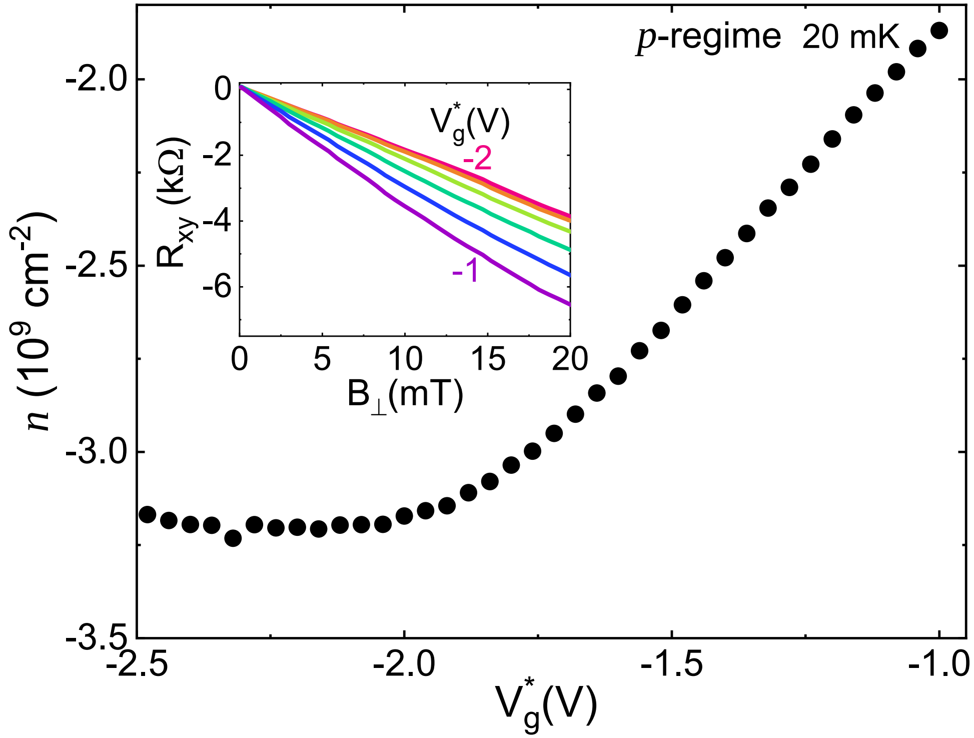

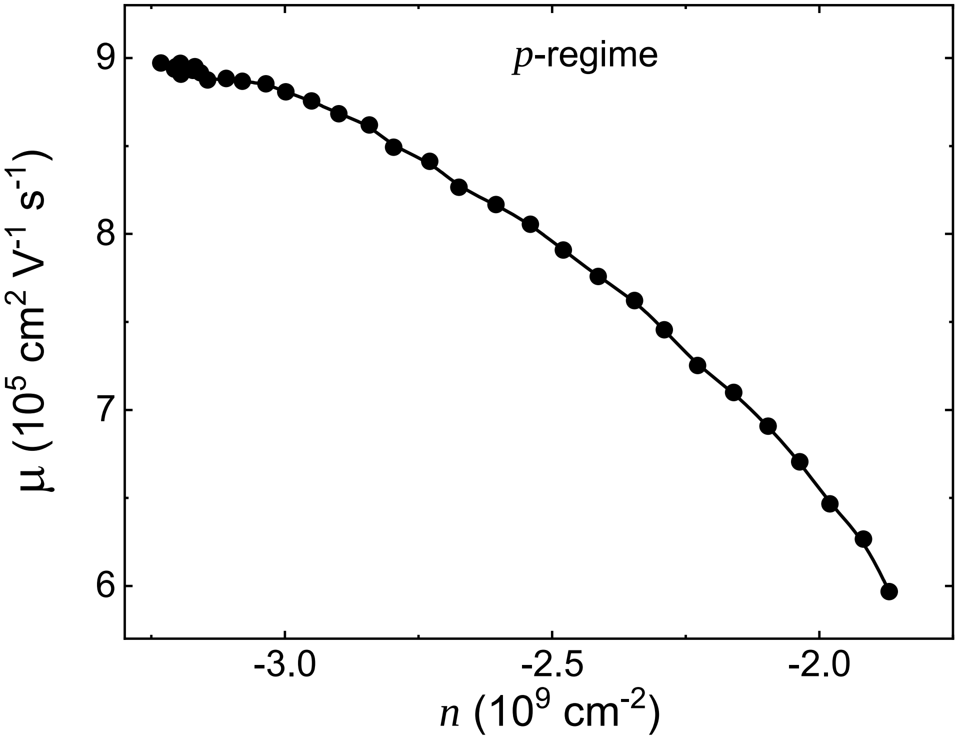

Localized carriers at the *camelback*

Extremely low density two dimensional system with *extremely* high mobility

Now in 3D TIs:
Topological and massive surface states

Two-dimensional massless electrons in an inverted contact

JETP Lett. **42**, 178 (1985)

B. A. Volkov and O. A. Pankratov
P. N. Lebedev Physics Institute, Academy of Sciences of the USSR

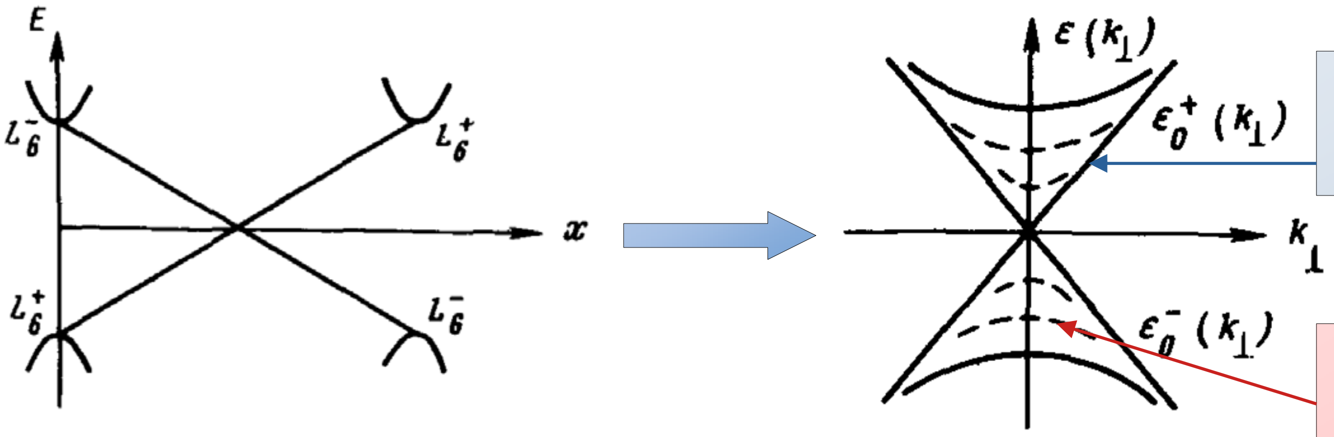

Topological surface states
(= **massless** VP states)

Trivial surface states
(= **massive** VP states)

FIG. 2. Energy spectrum of the inverted contact. Solid curves—The Dirac (band) state and the Weyl state; dashed curves—additional branches which arise when the contact thickness is $l > l_0$.

History

In hindsight, topological insulators were almost predicted in the mid-1980s and directly connected with the parity anomaly!

$$\sigma_{xy} = -\frac{1}{2}\frac{e^2}{h}\sum_i \chi_i \,\mathrm{sgn}(m_i)$$

$$= -\frac{1}{2}\frac{e^2}{h}[\mathrm{sgn}(m_1) - \mathrm{sgn}(m_2)]$$

(for two Dirac fermions)

- G. W. Semenoff, Phys. Rev. Lett. **53**, 2449 (1984).
- B. A. Volkov and O. A. Pankratov, JETP Lett. **42**, 178 (1985).
- F. V. Kusmartsev and A. M. Tsvelik, JETP Lett. **42**, 257 (1985).
- E. Fradkin, E. Dagotto, and D. Boyanovsky, Phys. Rev. Lett. **57**, 2967 (1986).
- F. D. M. Haldane, Phys. Rev. Lett. **61**, 2015 (1988).

Parity anomaly in condensed matter

Model for a single Dirac electron: (≈ ½ BHZ model)

$$H = \mathcal{C}\sigma_0 + m\sigma_z - \mathcal{A}(k_y\sigma_x - k_x\sigma_y) = \begin{pmatrix} \mathcal{C}+m & -\mathrm{i}\mathcal{A}k_- \\ \mathrm{i}\mathcal{A}k_+ & \mathcal{C}-m \end{pmatrix}$$

Dirac mass:
m > 0 normal
m < 0 inverted

parity anomaly
no gauge invt theory of single parity invariant Dirac particle in 2+1D

- G. W. Semenoff, Phys. Rev. Lett. **53**, 2449 (1984).
- E. Fradkin, E. Dagotto, and D. Boyanovsky,
- Phys. Rev. Lett. **57**, 2967 (1986).
- F. D. M. Haldane, Phys. Rev. Lett. **61**, 2015 (1988).

Spectral asymmetry

Dirac electron in a magnetic field B

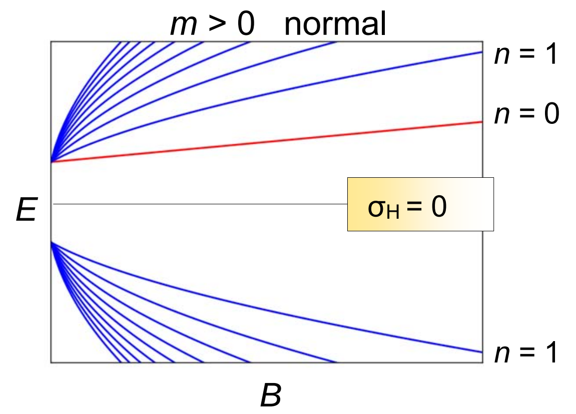

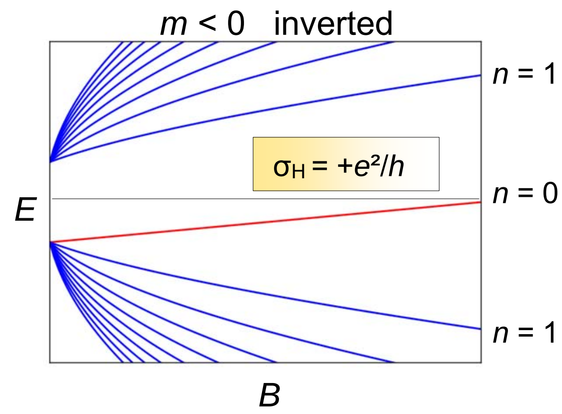

There is only a single zero Landau level (n = 0)

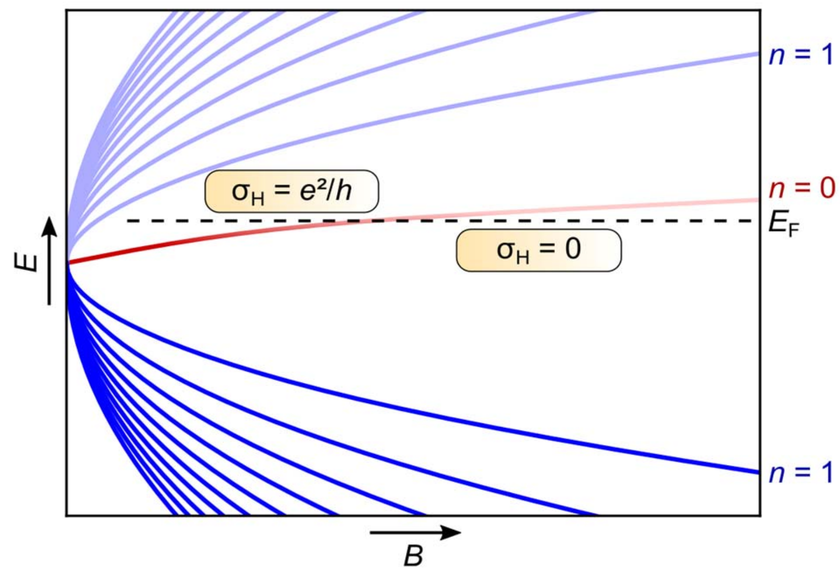

Spectral asymmetry

Normal band ordering → $\sigma_H = 0$

Inverted bands → $\sigma_H = +e^2/h$

Magnetotransport!

Experiment: Re-entrant QHE

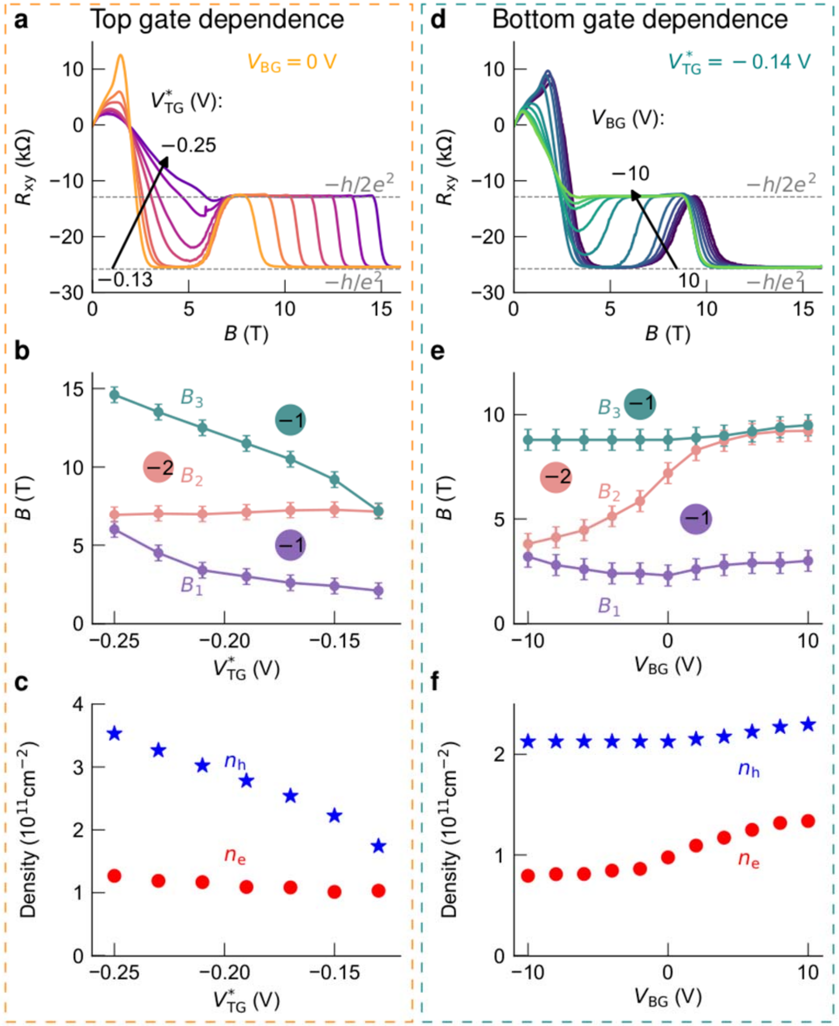

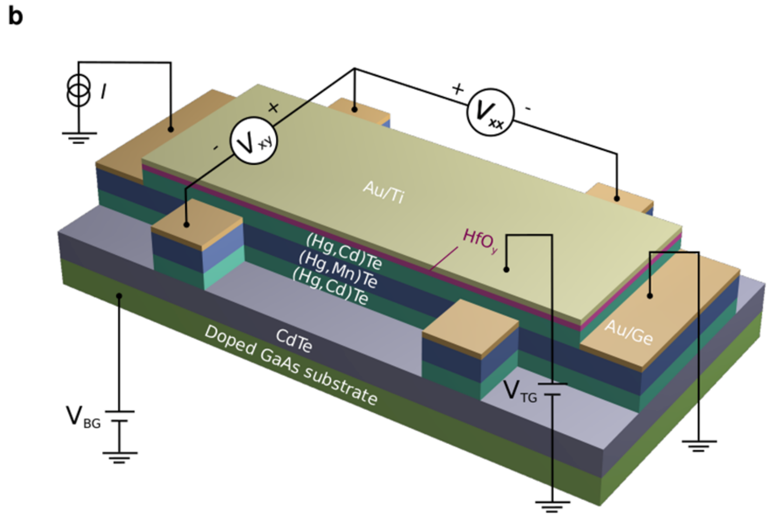

Lixian Wang, et al. (submitted)

Theoretical model: k·p theory + electrostatics

$U_{\mathrm{i}} = 50\,\mathrm{meV}$

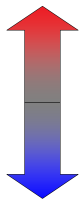

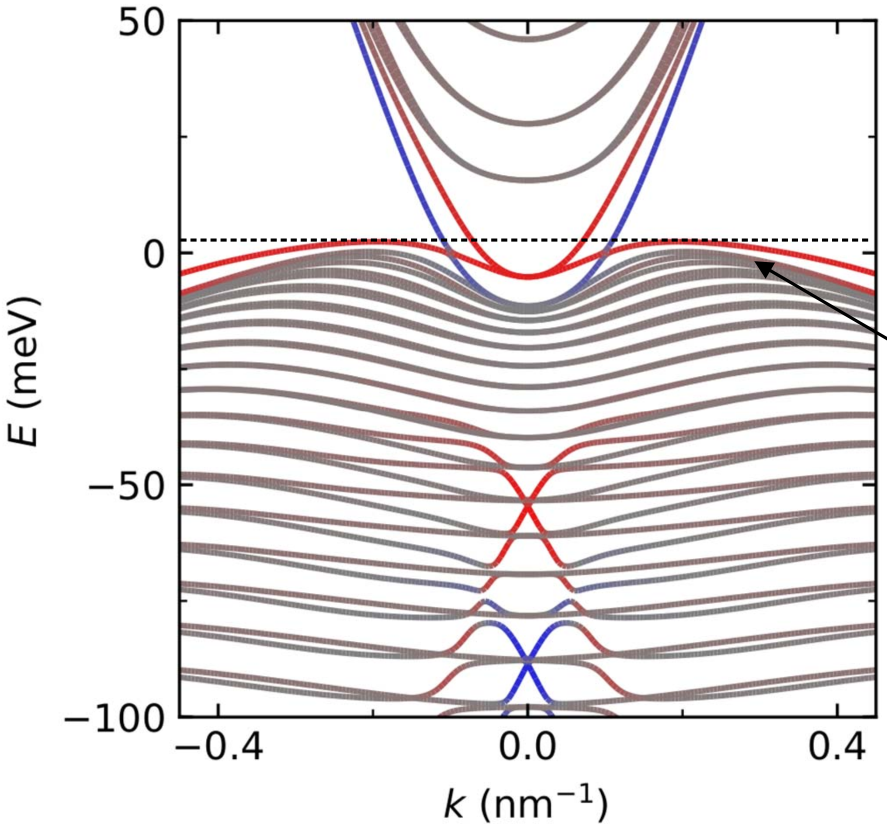

E_{F} → Fermi level **pinning**

New surface state appears:

Massive Volkov-Pankratov state

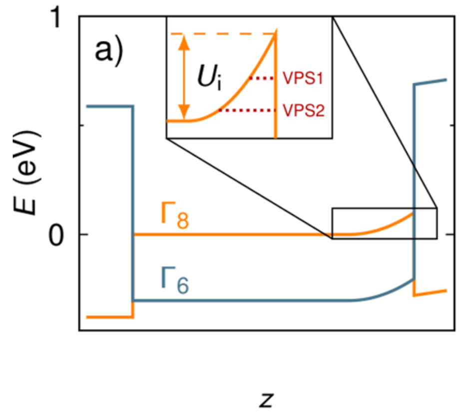

Re-entrant QHE due to Parity Anomaly

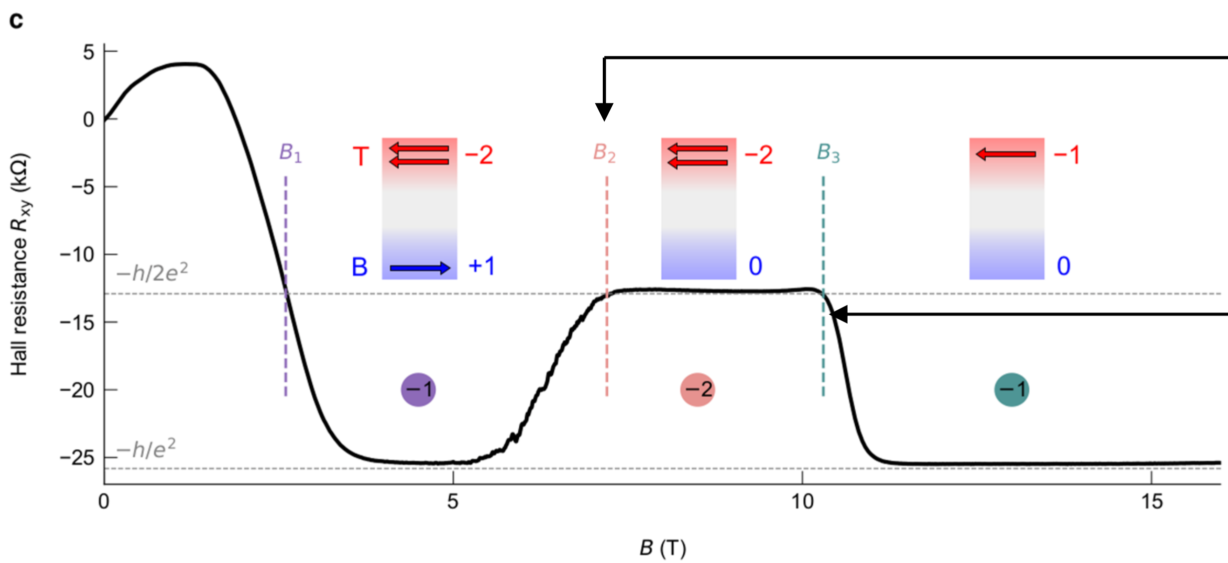

Topological state (B surf.)
$\Delta\sigma_H = -e^2/h$
spectral asymmetry

Massive VP state (T surf.)
$\Delta\sigma_H = +e^2/h$
regular p-type QH transition

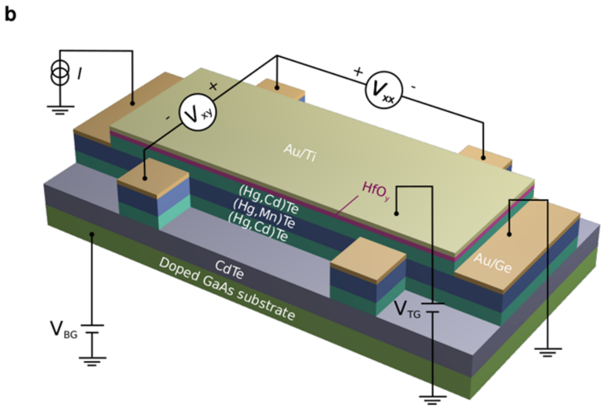

Hall bar with
top and bottom gates

Lixian Wang, et al. (submitted)

Dilute magnetic topological insulator based Josephson junctions

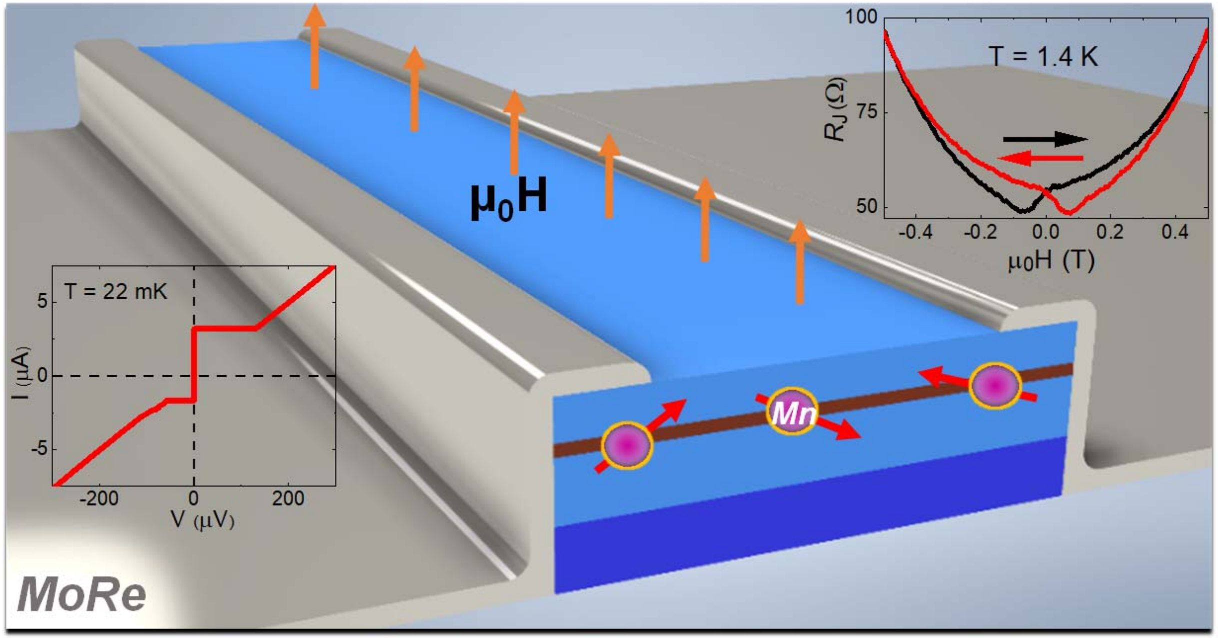

- 11 nm thick quantum well (QW), 2.3% Mn
- With MoRe side-contacted Josephson junction

Mandal et al., Nano Letters **22**, 3557 (2022)

Fraunhofer indicates flux focusing

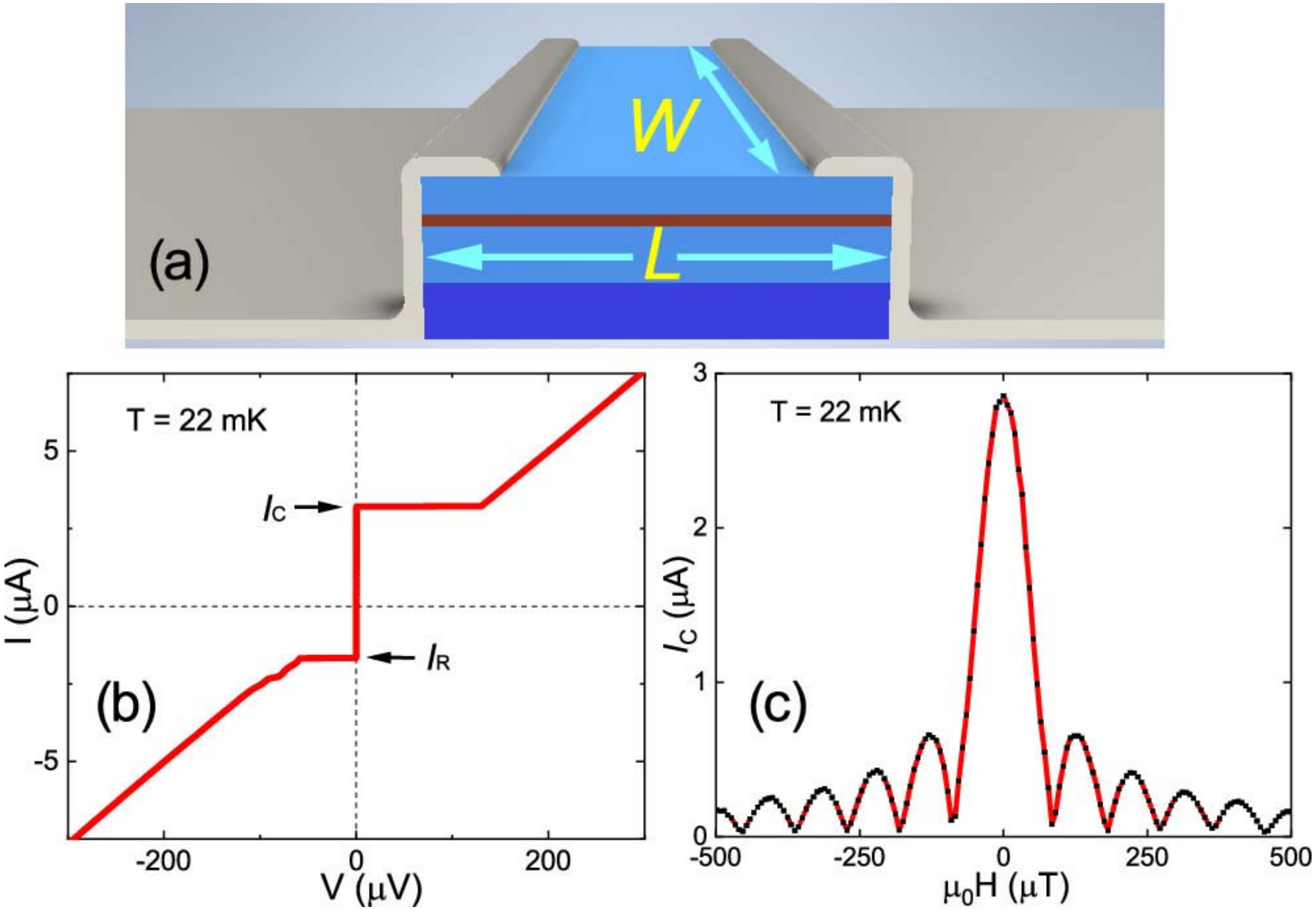

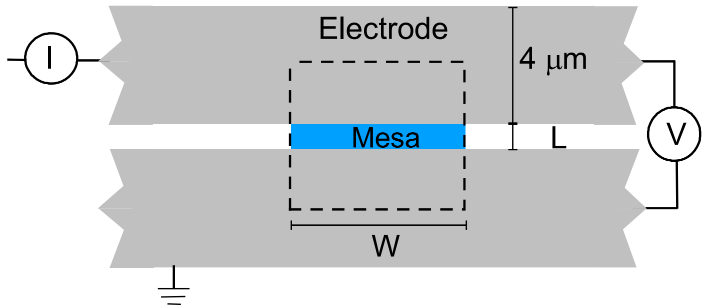

Flux period depends on area of the mesa plus flux focusing area from superconducting leads

With large magnetic field

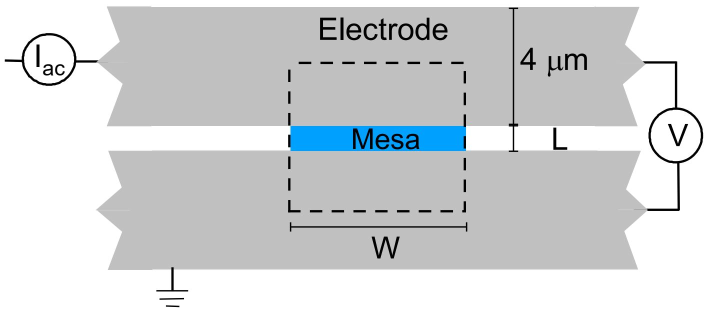

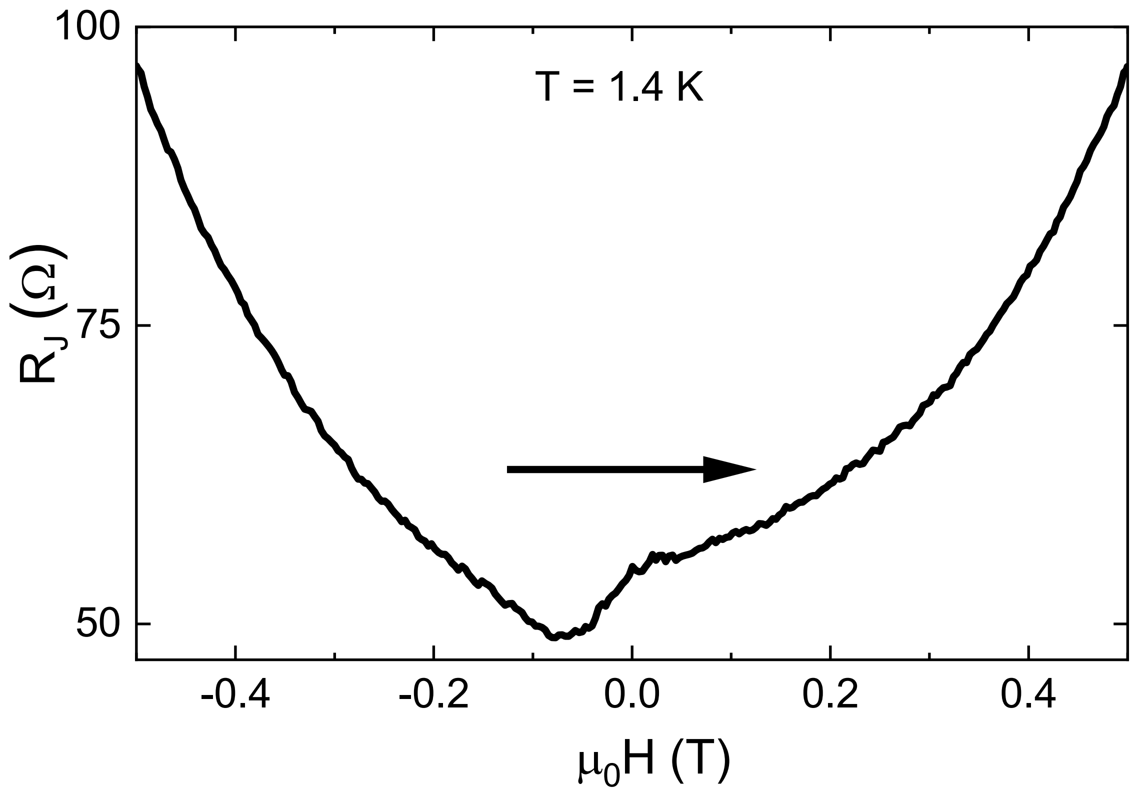

- Quasi 4-terminal measurement of the junction resistance with magnetic field sweep from left, reveals resistance minimum before reaching 0T !?

Flux focusing causes anti-hysteric response at high fields

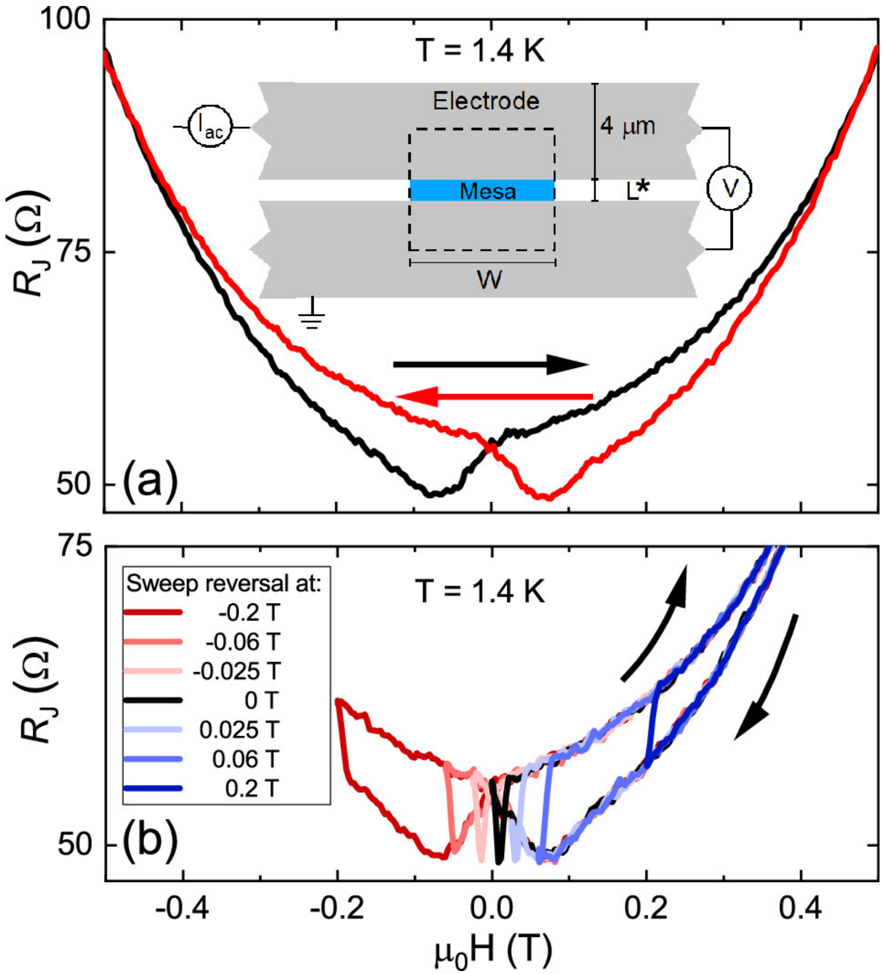

- Junction resistance reveal fields sweep direction dependent magneto-resistance
- Even switching behaviour
- Magnetic hysteresis of type-II superconductor can be understood based on Bean's critical state model from the 1960s

p-FFLO in a magnetic topological insulator

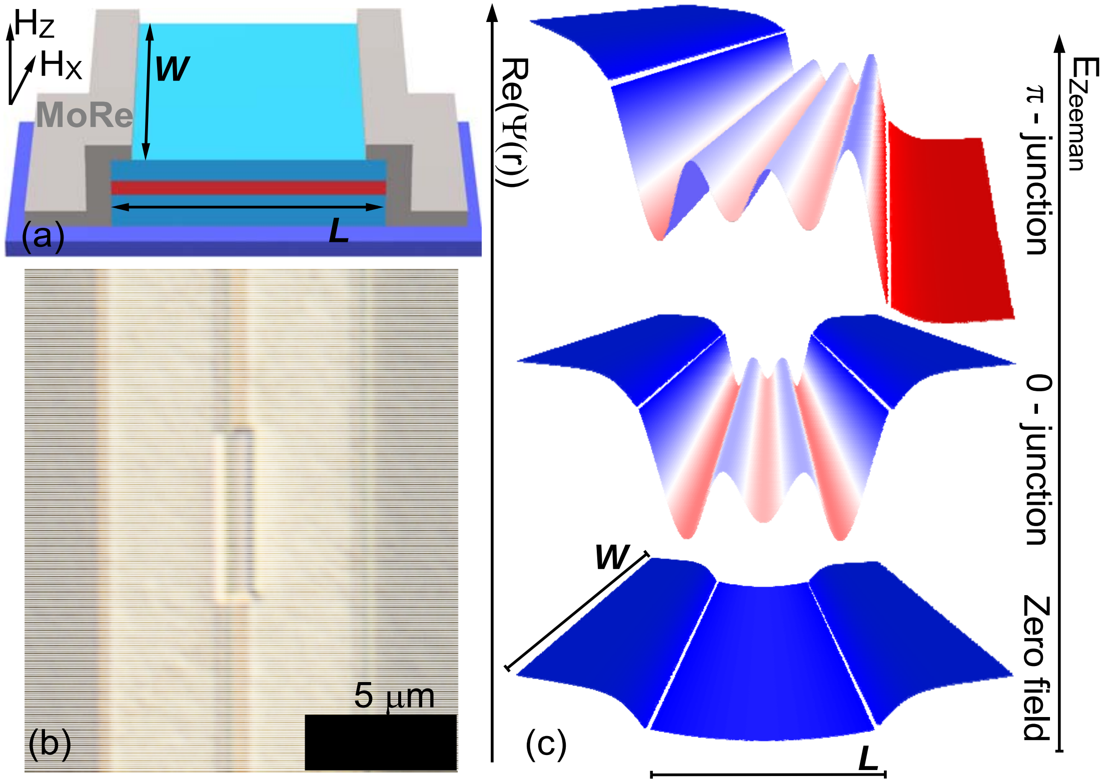

- Fulde-Ferell-Larkin-Ovchinnikov predicted oscillating order parameter at large Zeeman splitting.
- Plenty large Zeeman in (Hg,Mn)Te

- 11 nm thick quantum well (QW), 2.3% Mn (giant-Zeeman effect)
- QW embedded in (Cd,Hg)Te buffer layer, negligible Rashba spin-orbit coupling
- With MoRe side-contacted Josephson junction
- Device length (*L*) below bulk mean free path (1.7 μm)
- Nomarski image of device
- p-FFLO: Spatially oscillating effective order parameter induced in the QW with increase in Zeeman energy

Julius-Maximilians-
UNIVERSITÄT
WÜRZBURG

Induced supercurrent and Fraunhofer pattern

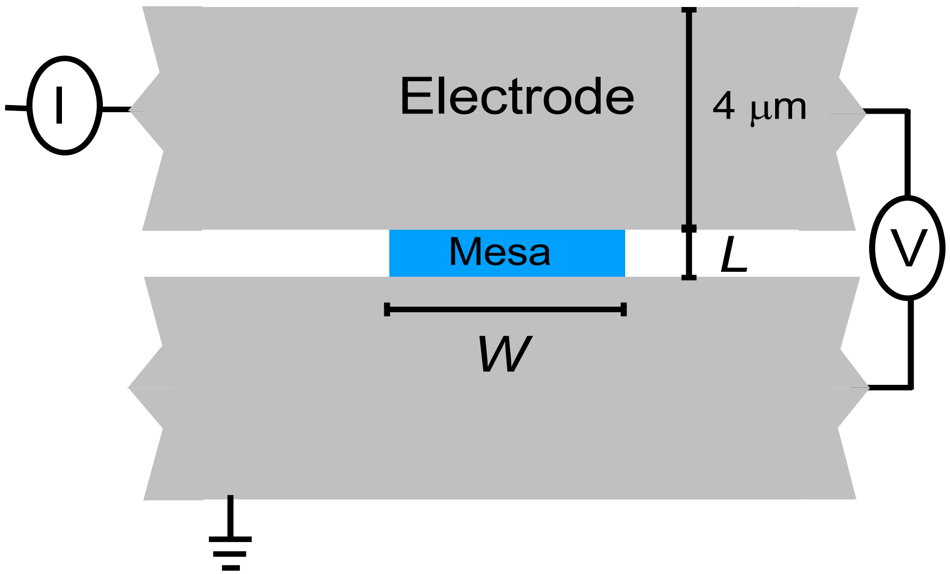

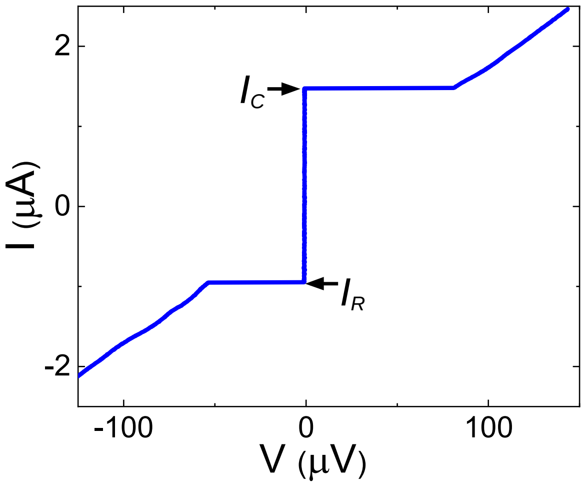

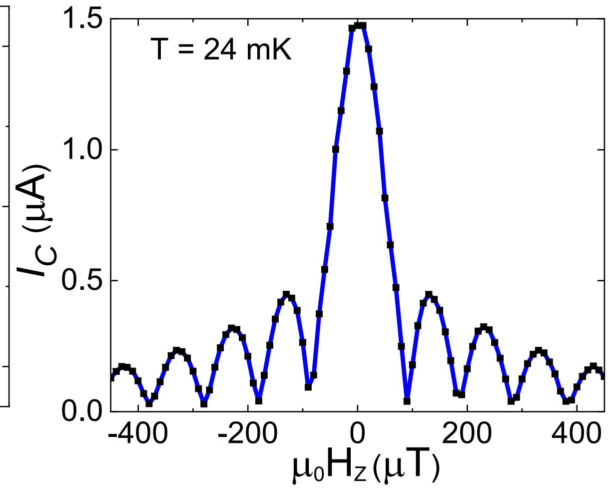

- DC measurement scheme
- I(V) characteristic at zero magnetic field
- I_c extracted using 2 μV voltage criterion
- Fraunhofer pattern I_c (H_z)
- H_z below MoRe H_{c1}

I(V) characteristics depend on in-plane field

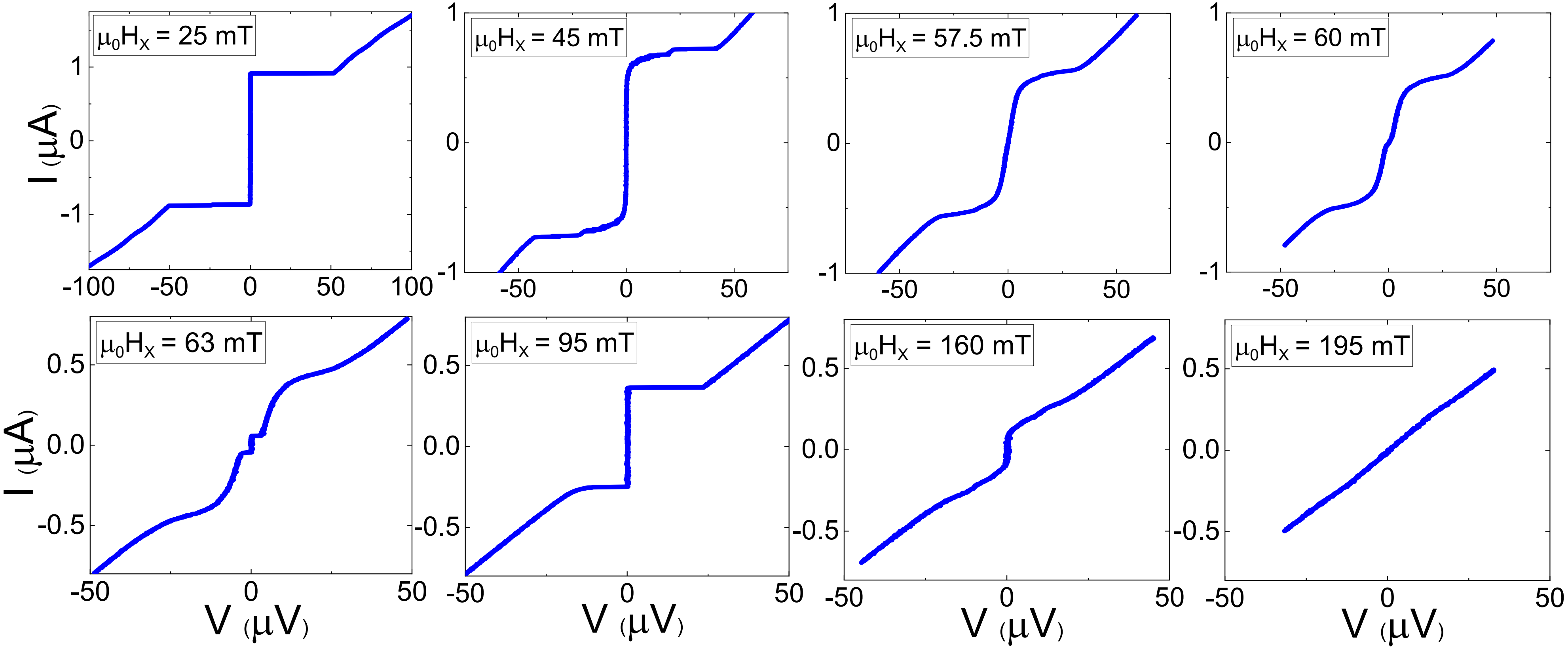

Pankaj Mandal, et al. (submitted)

I_C dependence on magnetic field

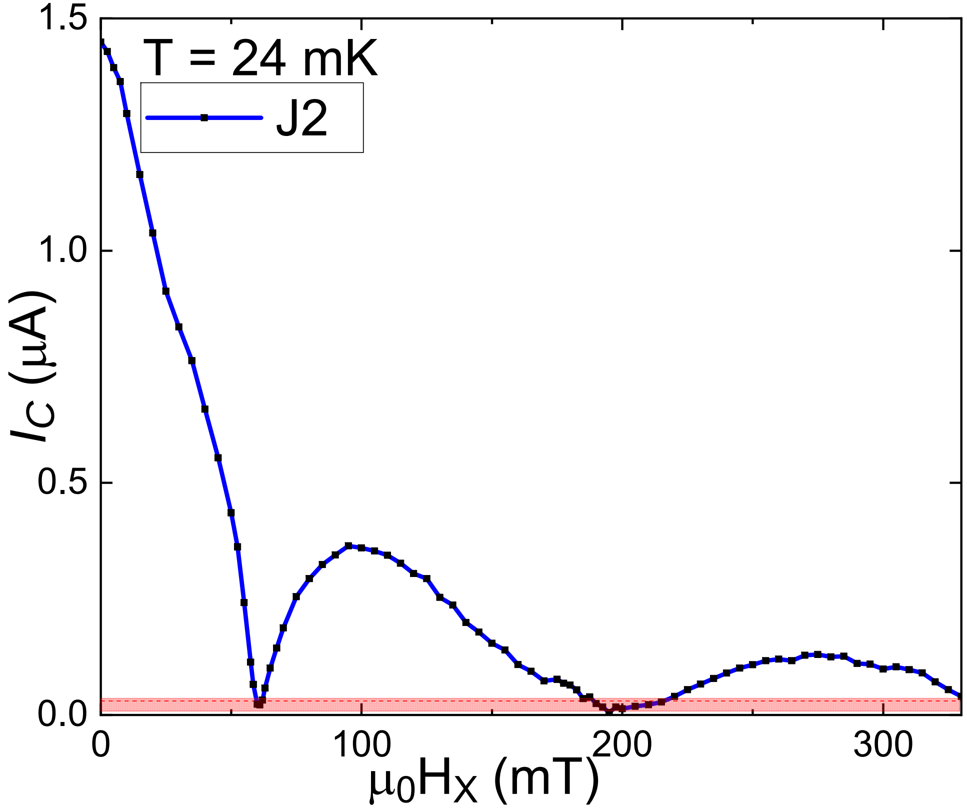

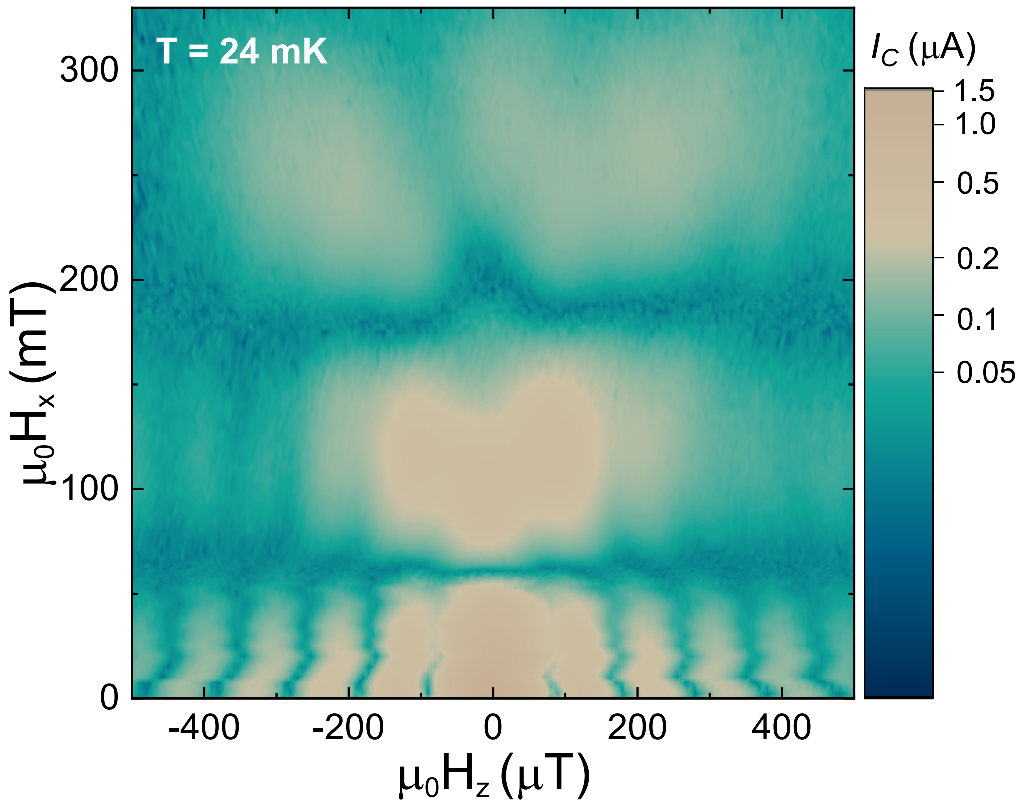

- Red shaded region: 2 μV voltage criterion sets a threshold of 30 nA (for 60 Ω junction resistance) on the I_C sensitivity of the measurement
- I_C goes to zero independent of out-of-plane field

I_C dependence on temperature

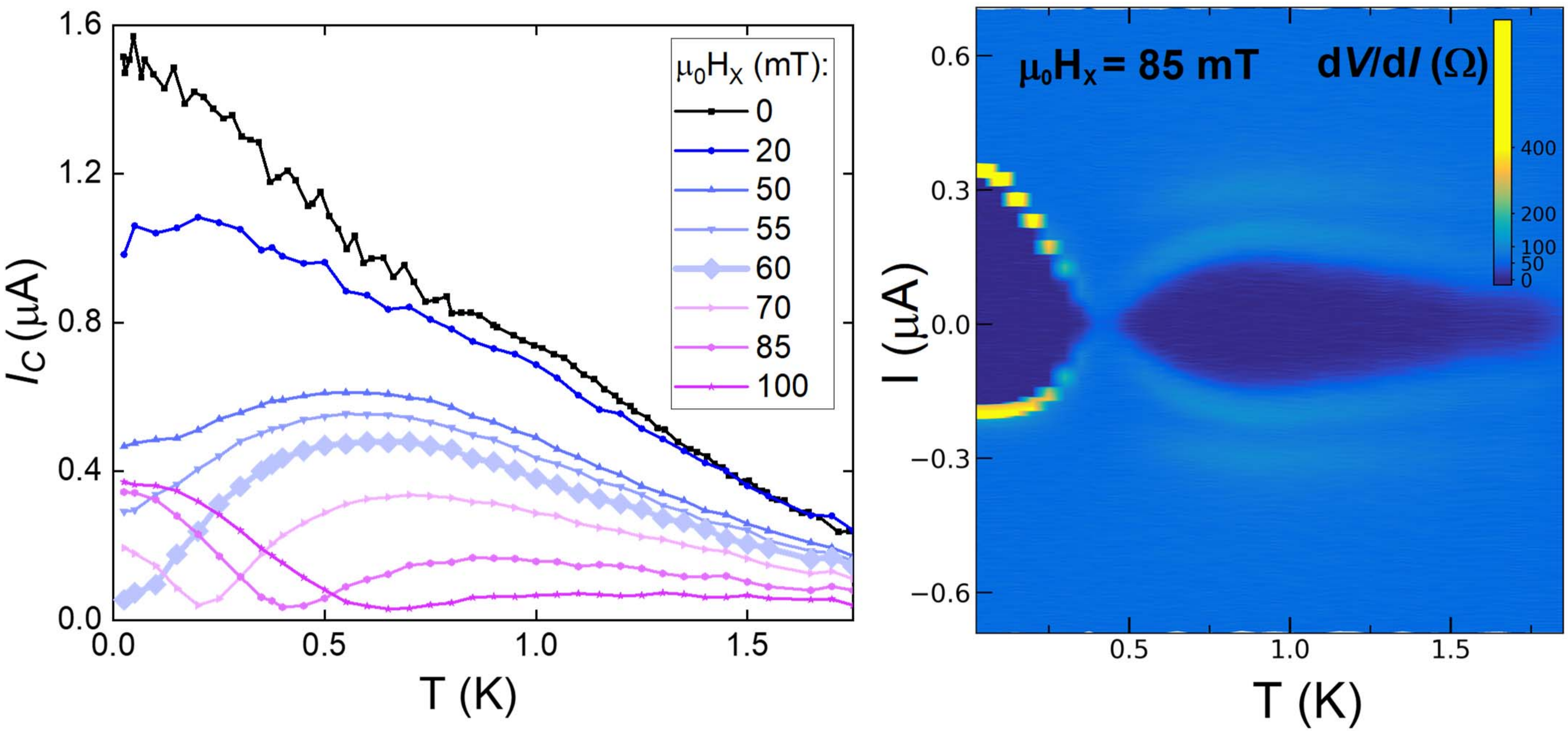

- Giant Zeeman depends on temperature, should show up in temperature dependence of I_c
- We plot temperature dependence of I_c for various in-plane fields
- Reentrance with change in temperature (dark blue area is zero resistance region)

Pankaj Mandal, et al. (submitted)

Reentrant behaviour in both in-plane field and temperature fits p-FFLO model

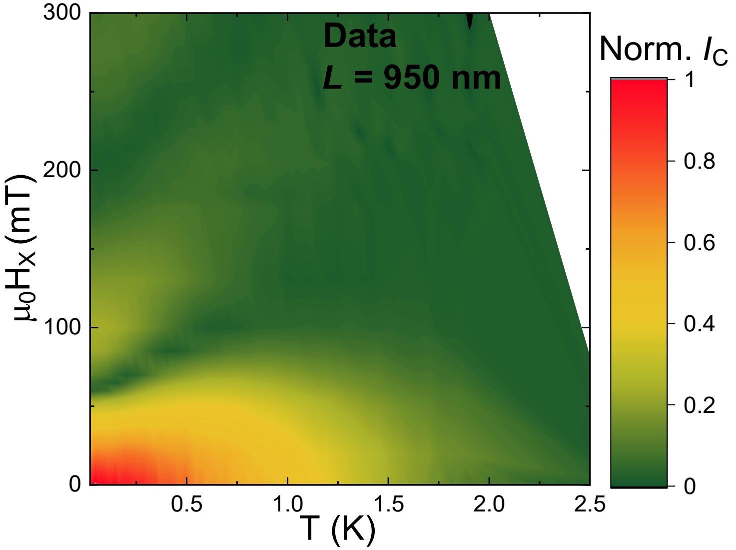

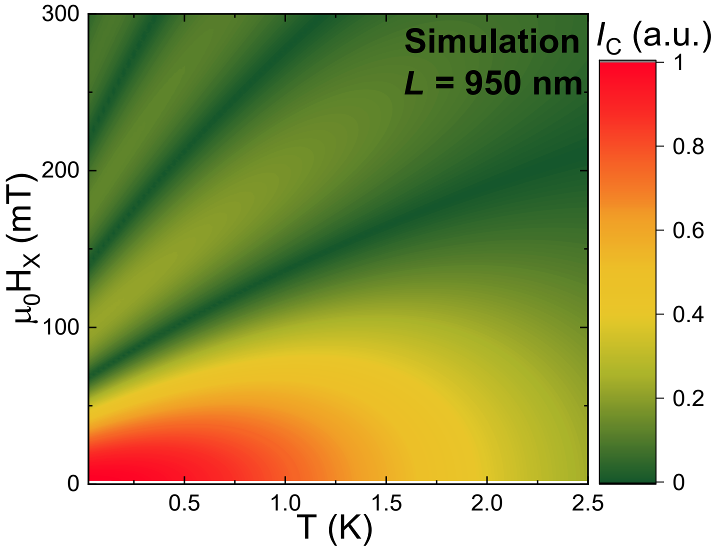

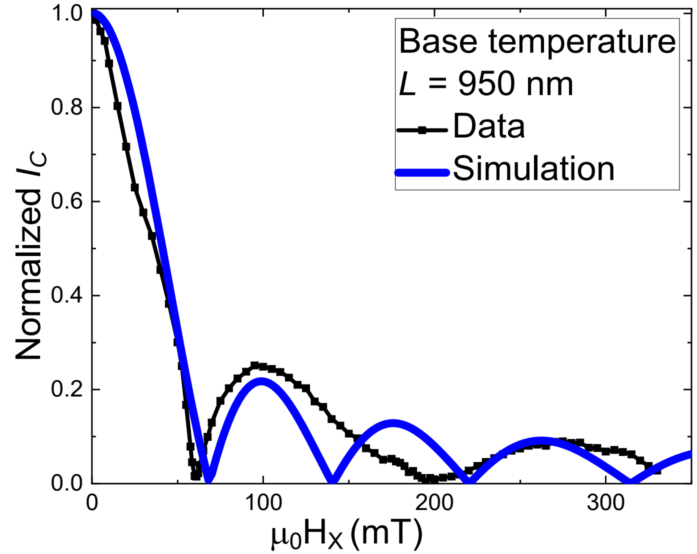

- Field and temperature dependence of I_C can be modelled based on theory developed for S/F/S junctions [Bergeret et al., PRB **64** (2001)], where exchange field is replaced by Zeeman
- In our case giant-Zeeman effect (E^*_Z) due to interacting Mn atoms resulting in field and temperature dependent Zeeman effect
- Also explains the shifting of the reentrance nodes towards lower fields at lower temperatures

$$E_Z^* = g_0\mu_B\mu_0H - \Delta E_{max}B_{5/2}\left[\frac{5g_{Mn}\mu_B\mu_0H}{2k_B(T+T_0)}\right],\qquad I_C \propto T\left|\sum_{\omega>0}^{\infty} f_s^2\gamma^2\frac{sin(2E_Z^*L/\hbar v_F)}{2E_Z^*L/\hbar v_F}e^{\frac{-L}{l}(1+2\omega\tau)}\right|.$$

Pankaj Mandal, et al. (submitted)

Summary and Outlook

- ✓ Quantum spin Hall effect survives Mn doping due to Kondo screening
- ✓ Emergence of $\nu = -1$ quantum Hall state at exceptionally low magnetic fields when chemical potential is in the bulk gap.
- ✓ In 3D device we observe a signature of the parity anomaly.
- ✓ Proximitized layers exhibit (p-)FFLO behaviour.

Collaborators: Pankaj Mandal, Saquib Shamim, Lixian Wang, Wouter Beugeling, Hartmut Buhmann, Charles Gould, Martin Stehno, Ewelina Hankiewicz, Björn Trauzettel
Sebastian Bergeret (San Sebastian), Teun Klapwijk (Delft)
Funding: Freistaat Bayern (ITI), DFG (SFB 1170, ct.qmat CoE), EU-ERC AGs “3 -TOP”, “4 TOPS”,